HHS Public Access

Author manuscript

Circulation. Author manuscript; available in PMC 2025 September 10.

Published in final edited form as:

Circulation. 2024 September 10; 150(11): 867–883. doi:10.1161/CIRCULATIONAHA.124.068624.

Skeletal Muscle SIRT3 Deficiency Contributes to Pulmonary Vascular Remodeling in Pulmonary Hypertension Due to Heart Failure with Preserved Ejection Fraction

Jia-Rong Jheng, PhD[1], **Yang Bai, PhD**[1,2], **Kentaro Noda, PhD**[3], **Joshua R. Huot, PhD**[4], **Todd Cook, BS**[1], **Amanda Fisher, BS**[1], **Yi-Yun Chen, PhD**[5], **Dmitry A. Goncharov, BS**[6], **Elena A. Goncharova, PhD**[6], **Marc A. Simon, MD**[7], **Yingze Zhang, PhD**[8], **Daniel E. Forman, MD**[9,10], **Mauricio Rojas, MD**[11], **Roberto F. Machado, MD**[1,4], **Johan Auwerx, PhD**[12], **Mark T. Gladwin, MD**[13], **Yen-Chun Lai, PhD**[1,4]

[1]Division of Pulmonary, Critical Care, Sleep and Occupational Medicine, Indiana University School of Medicine, Indianapolis, IN, USA

[2]Department of Clinical Pharmacology, School of Pharmacy, China Medical University, Shenyang, China

[3]Department of Cardiothoracic Surgery, University of Pittsburgh Medical Center, Pittsburgh, PA, USA

[4]Department of Anatomy, Cell Biology and Physiology, Indiana University School of Medicine, Indianapolis, IN, USA

[5]Institute of Biological Chemistry, Academia Sinica, Taipei, Taiwan

[6]Division of Pulmonary, Critical Care and Sleep Medicine, University of California Davis, Davis, CA, USA

[7]Division of Cardiology, University of California San Francisco, San Francisco, CA, USA

[8]Division of Pulmonary, Allergy and Critical Care Medicine, University of Pittsburgh, Pittsburgh, PA, USA

[9]Department of Medicine, Divisions of Geriatrics and Cardiology, University of Pittsburgh, Pittsburgh, PA, USA

Address correspondence to: Yen-Chun Lai, Division of Pulmonary, Critical Care, Sleep and Occupational Medicine, Indiana University School of Medicine 980 W. Walnut St. R3 C412, Indianapolis, Indiana 46202; yelai@iu.edu.

Author Contributions

JRJ, YB, KN, YYC, and YCL developed methodology, performed experiments, and analyzed data. JRH helped with skeletal muscle cells experiments. TC and AF performed echocardiogram and/or hemodynamic measurements. DAG performed lung histology analysis in *Sirt3*$^{skm-/-}$ mice. EAG provided human PASMCs from obese and non-obese subjects. MAS provided muscle biopsies and plasma samples from patients with PH-HFpEF. YZ provided plasma samples from healthy control subjects. DEF provided muscle biopsies from HFpEF patients. MR assisted with PCLS experiments. JA provided *Sirt3*-floxed mice. RFM and MTG supervised the study. YCL wrote the manuscript with input from all authors.

Disclosures

Dr. Gladwin is a co-inventor of patents and patent applications directed to the use of recombinant neuroglobin and heme-based molecules as antidotes for CO poisoning, which have been licensed by Globin Solutions, Inc. Dr. Gladwin is a shareholder, advisor, and director in Globin Solutions, Inc. Dr. Gladwin is also co-inventor on patents directed to the use of nitrite salts in cardiovascular diseases, which were previously licensed to United Therapeutics, and is now licensed to Globin Solutions and Hope Pharmaceuticals. Dr. Gladwin is a principal-investigator in an investigator-initiated research study with Bayer Pharmaceuticals to evaluate riociguate as a treatment for patients with SCD.

[10]Geriatric Research, Education, and Clinical Center (GRECC), VA Pittsburgh Healthcare System, Pittsburgh, PA, USA

[11]The Ohio State University, Columbus, OH, USA

[12]Laboratory of Integrative Systems Physiology, Ecole Polytechnique Fédérale de Lausanne, Lausanne, Switzerland

[13]Department of Medicine, University of Maryland, Baltimore, MD, USA

Abstract

Background: Pulmonary hypertension (PH) is a major complication linked to adverse outcomes in heart failure with preserved ejection fraction (HFpEF), yet no specific therapies exist for PH associated with HFpEF (PH-HFpEF). We have recently reported on the role of skeletal muscle sirtuin-3 (SIRT3) in modulation of PH-HFpEF, suggesting a novel endocrine signaling pathway for skeletal muscle modulation of pulmonary vascular remodeling. In this study, we attempted to define the processes by which skeletal muscle SIRT3 defects affect pulmonary vascular health in PH-HFpEF.

Methods and Results: Notably, skeletal muscle-specific *Sirt3* knockout mice ($Sirt3^{skm-/-}$) exhibited reduced pulmonary vascular density accompanied by pulmonary vascular proliferative remodeling and elevated pulmonary pressures. Using mass spectrometry-based comparative secretome analysis, we demonstrated elevated secretion of lysyl oxidase homolog 2 (LOXL2) in SIRT3-deficient skeletal muscle cells. Elevated circulation and protein expression levels of LOXL2 were also observed in plasma and skeletal muscle of $Sirt3^{skm-/-}$ mice, rat model of PH-HFpEF, and in humans with PH-HFpEF. Additionally, expression levels of canopy fibroblast growth factor signaling regulator 2 (CNPY2), a known proliferative and angiogenic factor, were increased in pulmonary artery endothelial cells (PAECs) and pulmonary artery smooth muscle cells (PASMCs) of $Sirt3^{skm-/-}$ mice and animal models of PH-HFpEF. CNPY2 levels were also higher in PASMCs of subjects with obesity compared to non-obese subjects. Moreover, treatment with recombinant LOXL2 protein promoted PAECs migration/proliferation and PASMCs proliferation via regulation of CNPY2-p53 signaling. Finally, skeletal muscle-specific *Loxl2* deletion decreased PAECs and PASMCs expression of CNPY2 and improved pulmonary pressures in mice with high-fat diet (HFD)-induced PH-HFpEF.

Conclusions: This study demonstrates a systemic pathogenic impact of skeletal muscle SIRT3 deficiency in remote pulmonary vascular remodeling and PH-HFpEF. This study suggests a new endocrine signaling axis that links skeletal muscle health and SIRT3 deficiency to remote CNPY2 regulation in the pulmonary vasculature through myokine LOXL2. Our data also identify skeletal muscle SIRT3, myokine LOXL2, and CNPY2 as potential targets for the treatment of PH-HFpEF.

Introduction

One-half of approximately six million heart failure patients in the United States are estimated to suffer from heart failure with preserved ejection fraction (HFpEF).[1,2] Among those, roughly half (23 to 83%) have pulmonary hypertension (PH, Group 2, PH-HFpEF), imposing an economic burden of about 8 billion per annum.[3–6] PH-HFpEF is a multifactorial syndrome with a range of disease entities (e.g. combined pre- and

post-capillary PH; Cpc-PH, isolated post-capillary PH; Ipc-PH, and likely others).[7] Obesity, diabetes, sedentary lifestyle, and hypertension are commonly observed and, compounded by the effects of aging, confer increased risk of PH-HFpEF.[3,8–10] Qualitative studies have documented that patients with PH-HFpEF develop more severe symptoms than those with HFpEF and suffer significant exercise intolerance, frequent hospitalization, and reduced survival.[8] While many patients with HFpEF develop pathological pulmonary vascular remodeling and are at higher risk of death than those without intrinsic pulmonary vascular disease, the mechanisms leading to these disproportionate changes in the pulmonary vasculature remain unclear.

Studies by our group and others have shown that the metabolic syndrome exacerbates PH-HFpEF via impaired nitric oxide (NO)-soluble guanylate cyclase signaling, increased epidermal growth factor receptor (EGFR) expression, elevated levels of proinflammatory cytokine interleukin-6 (IL-6), and activated signal transducer and activator of transcription 3 (STAT3)-signaling in the pulmonary vasculature.[11–14] Aside from the lung, increased expression of natriuretic peptide receptor C (NPRC) and lipid accumulation in the right ventricle (RV), as well as enhanced platelet maximal respiratory capacity, have been correlated with RV dysfunction in PH-HFpEF.[15–17] Elevated circulation levels of interleukin-1 beta (IL-1β), endothelin-1 (ET-1), and leptin, an adipokine which is known to induce secretion of proinflammatory cytokines and reactive oxygen species (ROS) generation, and reduced plasma levels of cardioprotective adipokine adiponectin, have also been associated with PH severity in humans and in animal models of PH-HFpEF.[11,14,18–22] Moreover, low plasma levels of cyclic 3’5’ guanosine monophosphate (cGMP), which mediates vasodilation, and reduced pulmonary artery (PA) expression of soluble guanylate cyclase b1 subunit (sGCβ1), which generates cGMP, were found to be associated with increased ROS production and PA dysfunction in SU5416-exposed obese ZSF1 rats (Ob-Su) during exercise.[23]

Growing evidence suggests that pulmonary vascular pathology in PH-HFpEF is multifactorial and involves complex systemic alterations contributed by multiple organs, such as skeletal muscle, adipose tissue, and kidney.[24–27] Defects in skeletal muscle (e.g. reduced type I oxidative fibers, impaired mitochondrial function, and insulin resistance) are associated with severe exercise intolerance and worsening functional capacity in patients with PH-HFpEF.[28–30] Using the Ob-Su rat model of PH-HFpEF, we recently reported that the level of sirtuin-3 (SIRT3), the mitochondrial deacetylase which is critical for modulating metabolic syndrome, PH, and aging,[31–33] is decreased predominantly in skeletal muscle, but not in the pulmonary vasculature, heart, or liver; concomitant with a robust increase in pulmonary pressures and pulmonary vascular remodeling.[11] Restoration of SIRT3 in skeletal muscle with nitrite (a drug that is metabolized to NO) and metformin (the first-line drug for metabolic syndrome) improved disease phenotypes, indicating a critical role of skeletal muscle SIRT3 in regulating pulmonary vascular remodeling and PH-HFpEF.[11] However, mechanistic understanding regarding the nature of molecular regulation, with respect to skeletal muscle SIRT3 deficiency and remote pulmonary vascular remodeling, remains unclear. In this study, using skeletal muscle-specific *Sirt3* knockout mice (*Sirt3*$^{skm-/-}$), together with mass spectrometry-based comparative secretome analysis and *ex vivo* precision-cut lung slices (PCLS), a dynamic organ culture system that mimics *in vivo* lung

tissue physiology,[34] we explore the mechanistic basis of the cross-organ communications and attempt to define the processes by which skeletal muscle SIRT3 defects affect pulmonary vascular health in PH-HFpEF.

Material and Methods

All data supporting the findings of this study is available from the corresponding author upon a reasonable request. Detailed methods and materials are available in the Data Supplement. Methods include generation of PCLS, pulmonary vascular structure measurements, cell cultures, mass spectrometry experiments, western blot analysis, plasmid construction, cell proliferation and migration assays, ELISA, treatment of β-aminopropionitrile (BAPN) in rat model of PH-HFpEF, and glucose tolerance test.

Animals

Sirt3-floxed mice (C57BL/6N background) were provided by Dr. Johan Auwerx and were crossed with mice expressing *Cre* recombinase under the control of a human α-skeletal actin promoter (HSA-*Cre*; #006149, C57BL/6 background; The Jackson Laboratory) to obtain $Sirt3^{skm-/-}$ mice.[35] *Loxl2*-floxed mice (mixed C57BL/6;FVB background) were provided by Dr. Amparo Cano and were crossed with mice expressing *Cre* recombinase under the control of the muscle creatine kinase promoter (MCK-*Cre*; #006475,C57BL/6 background; The Jackson Laboratory) to obtain $Loxl2^{skm-/-}$ mice.[36] Beginning at 8 weeks of age, male, female, and their littermate wild-type (WT) control mice were randomly fed a high-fat diet (HFD; 60% lipids/kcal, #D12492, Research Diets) or regular diet (RD; 10% lipids/kcal, #D12450J, Research Diets) for 16 weeks. All experimental procedures were approved by Indiana University School of Medicine Institutional Animal Care and Use Committee and the University of Pittsburgh Institutional Animal Care and Use Committee. Animal studies reported in this article are in compliance with the ARRIVE guidelines. Sample size for 80% power at a significance level of 0.05 to detect a change in RVSP using power analyses suggests $n = 7$ mice/group (standard deviation of 1.6, effect size of 1.7). In all experiments, animals were randomly assigned to control and experimental groups. When measuring various parameters or performing assays, the order in which samples were processed or analyzed was randomized.

Hemodynamic Measurements

Animals were weighed and anesthetized with isoflurane (5% for induction, 2% during surgery, and 1% while performing pressure measurements). Right ventricular systolic pressure (RVSP), left ventricular (LV) end-diastolic pressure (LVEDP), and LV ejection fraction (LVEF) were measured using an admittance pressure-volume catheter. Weights of RV and LV+septum normalized to tibial length were used as indexes of ventricular mass. All measurements were performed blinded. Success rates of invasive RVSP and LVEDP measurements were 90% and 80%, respectively, across experiments – values typical for this level of experimental complexity and the main reason for missing data point. No data was excluded during analysis.

Microcomputed Tomography Angiography

Microcomputed tomography angiography (micro-CT) was performed to evaluate the pulmonary vessels in mice. The main PA was cannulated via the RV wall and blood was flushed from the lungs with phosphate-buffered saline (PBS, #10010–023, Gibco). Then, the lungs were perfused with contrast agent (Liquid Mercox II resin, Ladd Research Industries Inc.) including $CaCO_3$ nanoparticle (60 mg/ml). After confirming that the reagent was circulated in the entire lungs, the PA and ascending aorta were ligated to secure the reagent in the pulmonary vasculature. After solidification of the contrast agent, the lungs were removed from the body and fixed in 10% formalin. Fixed lungs were scanned using the Siemens Inveon Multimodality micro-CT scanner (Siemens Medical Solutions Inc., Knoxville, TN) set to 80 kVp/100 μA, and 3500 msec exposure at 45 μm resolution (45×45×45 μm/voxel).[37] The detector and X-ray source were rotated 220 degrees in 1-degree steps, calibration exposures configured to 20, and the field-of-view set at maximum voxel size of 50×50×50 mm^3. CT data were DICOM converted and examined using OsiriX DICOM Viewer (the OsiriX Foundation, Geneva, Switzerland). Scanned lung images were reconstructed into 3D images and used for volumetric analysis. All measurements were performed blinded.

Human Subjects and Ethical Considerations

De-identified human pulmonary artery smooth muscle cells (PASMCs) provided by Dr. Elena Goncharova were isolated, maintained, and characterized as previously described[38] under the protocols approved by the University of Pittsburgh Institutional Review Board. De-identified muscle biopsies and/or plasma samples of HFpEF and PH-HFpEF subjects participating in clinical trials (NCT02918552 and NCT03629340; all patients provided written informed consent before participating in the trials) were collected at baseline under protocols approved by the University of Pittsburgh Institutional Review Board and/or University of California San Francisco Institutional Review Board.

Statistical Analysis

Statistical analyses were performed using Prism 10.0.2 software (La Jolla, CA). Statistical comparison between two groups were performed using Mann-Whitney *U*-test or unpaired Student's *t*-test after testing for normality with Shapiro-Wilk test. Comparison among ≥ 3 groups was performed using one-way or two-way analysis of variance (ANOVA) followed by Tukey's *post hoc* test. For differences in blood glucose levels during the glucose tolerance test, two-way ANOVA followed by Bonferroni's *post hoc* test was performed. Values of $P < 0.05$ were considered statistically significant.

Results

Absence of SIRT3 in skeletal muscle leads to reduced pulmonary vascular density, increased pulmonary vascular remodeling, and elevated pulmonary pressures.

To evaluate the role of skeletal muscle SIRT3 in the regulation of pulmonary vascular remodeling and PH-HFpEF, we generated *Sirt3*$^{skm-/-}$ mice by crossing *Sirt3*-floxed mice, on a C57BL/6N genetic background, with HSA-*Cre* mice.[35] The expression of SIRT3

protein was efficiently ablated in soleus muscles of *Sirt3*$^{skm-/-}$ mice compared to WT mice, whereas no significant reduction of SIRT3 was observed in the liver, lung, LV, RV, and isolated PASMCs (Figure 1A and Figure S1A and S1B in the Data Supplement). At baseline, we found that *Sirt3*$^{skm-/-}$ mice had reduced pulmonary vascular density, with less continuous blood vessels and narrowed vascular lumen diameter compared to that in WT mice (Figure 1B and 1C). Additionally, *Sirt3*$^{skm-/-}$ mice had increased pulmonary vascular proliferative remodeling (Figure 1D and Figure S1C in the Data Supplement) and slightly higher RVSP (Figure 1E). Elevated LVEDP, LV hypertrophy, glucose intolerance, and preserved LVEF were also observed in *Sirt3*$^{skm-/-}$ mice, with no changes related to body weight, right heart hypertrophy, systolic blood pressures, and aortic remodeling (Figure 1F–1K and Figure S1D and S1E in the Data Supplement). Together, these data suggest that there exists a systemic pathogenic impact of skeletal muscle SIRT3 deficiency in remote pulmonary vascular remodeling and PH-HFpEF.

Absence of SIRT3 in skeletal muscle leads to elevated LOXL2 secretion.

One of the most important findings over the past two decades in the area of skeletal muscle research is the discovery that several proteins and peptides are produced and secreted by skeletal muscle. These so-called myokines play a role in communication with distant effector tissues and are identified as possible therapeutic targets to treat metabolism-related disorders.[39–41] Using nano capillary liquid chromatography electrospray ionization mass spectrometry (nLC-ESI-MS) and tandem mass tag (TMT) isobaric labels,[42] secreted proteins extracted from media conditioned by SIRT3-deficient C2C12 myotubes were processed for a mass spectrometry experiment in which secreted proteomes were comprehensively characterized and quantitatively compared (Figure 2A and 2B). On average, 60 known muscle-secreted proteins were identified. Among them, 13 proteins were found to be differentially secreted (greater or less than 1.2-fold) in response to the absence of SIRT3 (Figure 2C). From the proteins with elevated secretion identified in skeletal muscle SIRT3-deficient cells, we selected lysyl oxidase homolog 2 (LOXL2), periostin, and gremlin-1 (Grem1) for further validation because of their reported association with PH and/or heart failure.[43–47] Plasma from *Sirt3*$^{skm-/-}$ mice had significantly higher circulating levels of LOXL2, but not periostin and Grem1, compared to WT mice (Figure 3A–C). Soleus muscles of *Sirt3*$^{skm-/-}$ mice had higher levels of LOXL2 compared to WT mice (Figure 3D). LOXL2 levels were also significantly increased in plasma obtained from SU5416-exposed obese ZSF1 rats with PH-HFpEF (Figure 3E). No correlation between plasma LOXL2 levels and RVSP was observed in Ob-Su rats (Figure 3F). LOXL2 is a matrix enzyme which cross-links collagen and elastin.[48] It has been implicated in the development of several diseases, including lung fibrosis, liver fibrosis, cancer, PAH, and heart failure.[43,45,49] There are five enzymes in the lysyl oxidase family, lysyl oxidase (LOX) and LOX-like 1–4 (LOXL1–4), and all of them share a conserved enzymatic domain with divergent N-termini. While we observed increased protein abundance of LOXL2 in SIRT3-deficient C2C12 myotubes, protein abundance levels of LOX, LOXL1, and LOXL3 were not affected by silencing of SIRT3 (Figure 2D) and LOXL4 was not detected in our experiments.

To further assess the clinical relevance of our findings, we measured LOXL2 levels in plasma obtained from human patients with PH-HFpEF and non-PH-HFpEF control subjects. Consistent with our observations in *Sirt3*$^{\text{skm}-/-}$ mice and the rat model of PH-HFpEF, circulating levels of LOXL2 trended higher in humans with PH-HFpEF compared to non-PH-HFpEF control subjects (Figure 3G and Table S1 in the Data Supplement). Furthermore, muscle biopsies of PH-HFpEF patients had increased expression of LOXL2, accompanied by decreased levels of SIRT3 as compared to HFpEF subjects without PH (Figure 3H and 3I and Table S2 in the Data Supplement), supporting the clinical relevance of skeletal muscle SIRT3 deficiency and the induction/secretion of LOXL2 in PH-HFpEF.

Secretome of SIRT3-deficient skeletal muscle in remote regulation of CNPY2 in the pulmonary vasculature.

Very little is known about the molecular regulation of skeletal muscle SIRT3 deficiency and remote pulmonary vascular remodeling. LOXL2 has been reported to modulate pulmonary vascular remodeling via increased extracellular matrix (ECM) stiffening.[45,50] However, the underlying mechanisms regarding LOXL2 action inside pulmonary vascular cells are not fully understood. LOXL2 has also been reported to promote tumor progression via activation of IRE1-XBP1 pathway of the UPR, independent of both ECM stiffness and collagen organization.[51] Dysregulated IRE1-XBP1 is also linked to cardiomyocyte dysfunction in HFpEF.[52] To assess if IRE1 and XBP1 are affected by LOXL2 within the pulmonary vasculature, mouse *ex vivo* PCLS containing all lung cell types in the same ratios and with the same cell-cell and cell-matrix interactions as *in vivo* and which are increasingly used to study lung biology,[53] were treated with recombinant LOXL2 protein. While IRE1 and XBP1 were not detected in PCLS, LOXL2 treatment increased short active form of activating transcription factor 6 (p50-ATF6) and activating transcription factor 4 (ATF4), which are also branches of the UPR (Figure 4A and Figure S2A in the Data Supplement). In addition, LOXL2 treatment increased the levels of downstream target and upstream regulator of ATF4, C/EBP-homologous protein (CHOP) and canopy fibroblast growth factor signaling regulator 2 (CNPY2), respectively, in PCLS (Figure 4A and Figure S2A in the Data Supplement). Immunofluorescent staining of PCLS also revealed an increase in CNPY2 in the CD31-positive ($CD31^+$) endothelium and the α-smooth muscle actin-positive (α-SMA^+) layer after LOXL2 treatment (Figure 4B). As protein expression levels of CNPY2, but not ATF6, were significantly elevated in lungs of rat model of PH-HFpEF (Figure 4C and Figure S2C in the Data Supplement), we focused on CNPY2 for further investigation.

CNPY2 has been recently identified as a key initiator of the PERK-ATF4-CHOP pathway of the UPR.[54] It can be transcriptionally upregulated by CHOP in a forward-feed loop to further enhance the UPR signaling.[54] While it is not known whether CNPY2 contributes to PH-HFpEF pathogenesis, activation of PERK-CHOP has been observed in PAH patients and in rats with monocrotaline (MCT)-induced PH.[55] PERK inhibition has also been shown to attenuate pulmonary vascular remodeling in rats with MCT- or Su/hypoxia-induced PH.[55,56] To assess whether LOXL2 affects CNPY2 in pulmonary vascular cells, we treated cultured human pulmonary artery endothelial cells (PAECs) and PASMCs with recombinant LOXL2 protein. Our data showed that treatment with recombinant LOXL2 protein significantly increased CNPY2 protein content in PAECs and PASMCs (Figure 4D and 4E). Using

media conditioned by SIRT3-deficient C2C12 myotubes, we next assessed the involvement of skeletal muscle secretome in the regulation of CNPY2 in PAECs and PASMCs. Importantly, conditioned media from SIRT3-deficient C2C12 myotubes increased CNPY2 protein expression in PAECs and PASMCs (Figure 4F and 4G), indicating the impact of the skeletal muscle secretome in remote regulation of CNPY2 in the pulmonary vasculature. Elevated CNPY2 protein levels were observed in isolated PAECs and PASMCs, $CD31^+$/isolectin$^+$ endothelium, and α-SMA^+ layer of *Sirt3*$^{skm-/-}$ mice and Ob-Su rats (Figure 5A–5D and Figure S3 and S4 in the Data Supplement), in which SIRT3 levels were decreased predominantly in skeletal muscle in relation to increased LOXL2 levels in the circulation (Figure 3E),[11] but not in the pulmonary cells (Figure S5 in the Data Supplement). These data support an idea that skeletal muscle-secreted LOXL2 may be a critical signaling molecule regulating CNPY2 in the pulmonary vasculature. While the lack of PAECs, PASMCs, and/or lung biopsies from patients with PH-HFpEF limits our ability to assess the clinical relevance of our findings in human disease, using a body mass index (BMI) of 29 as a cut-off, we found that CNPY2 protein levels trended higher in PASMCs obtained from obese subjects than those from non-obese subjects (Figure 5E and 5F). Together, these data suggest the role of CNPY2 as a key target of skeletal muscle SIRT3-LOXL2 signaling in the pulmonary vasculature.

Treatment with LOXL2 induces PAECs migration/proliferation and PASMCs proliferation via regulation of CNPY2-p53 signaling.

Emerging data indicate that CNPY2, as an initiator of the PERK-CHOP arm of the UPR, may contribute to PASMCs proliferation and dysfunction.[55–57] CNPY2 has also been shown to promote tumorigenesis through the UPR-dependent repression of the tumor suppressor p53.[58] Given that reduced p53 expression exaggerates experimental PH and is found in patients with PAH, we decided to examine the functional consequences of increased CNPY2 and its impact on p53 in the pulmonary vasculature.[59,60] To explore the role and mechanism of CNPY2 in endothelial abnormalities and pulmonary vascular remodeling, we overexpressed CNPY2 in human PAECs and PASMCs. Overexpression of CNPY2 markedly increased cell migration and proliferation in association with reduced p53 in PAECs (Figure 6A–6C), whereas siRNA-mediated knock-down of CNPY2 increased p53 expression (Figure S6A in the Data Supplement). In addition, knock-down of p53 significantly increased cell migration and proliferation in PAECs (Figure S6B–D in the Data Supplement). Moreover, treatment with recombinant LOXL2 protein reduced p53 expression in human PAECs (Figure 6D). Treatment with LOXL2 also significantly increased cell migration and proliferation in PAECs (Figure 6E and 6F). Notably, the ability of LOXL2 to increase PAECs migration and proliferation was reduced by knock-down of CNPY2 and overexpression of p53 (Figure 6E and 6F and Figure S6E and S6F in the Data Supplement).

In PASMCs, CNPY2 overexpression increased cell proliferation in association with decreased p53, whereas knock-down of CNPY2 increased p53 expression (Figure 6G–6I and Figure S7A in the Data Supplement). Knock-down of p53 increased proliferation in PASMCs (Figure S7B and S7C in the Data Supplement). Furthermore, human PASMCs treated with LOXL2 showed lower p53 protein content and increased cell proliferation, which was significantly decreased by knock-down of CNPY2 and overexpression of p53

(Figure 6J–L and Figure S7D in the Data Supplement). Together, these data suggest that LOXL2 induces PAECs migration and promotes PAECs and PASMCs proliferation via regulation of CNPY2-p53 signaling.

Skeletal muscle-specific LOXL2 deletion reduces PAECs/PASMCs expression of CNPY2 and improves pulmonary pressures in mice with HFD-induced PH-HFpEF.

To further evaluate skeletal muscle SIRT3 deficiency and its downstream LOXL2-mediated endocrine signaling in remote pulmonary vascular remodeling and PH-HFpEF, we generated skeletal muscle-specific *Loxl2* knockout mice. Of note, we observed non-specific deletion of LOXL2 when crossing *Loxl2*-floxed mice with HSA-*Cre* mice, thus MCK-*Cre* mice were used to generate $Loxl2^{skm-/-}$ mice. Western blot analyses showed that LOXL2 protein was specifically ablated in soleus muscles of $Loxl2^{skm-/-}$ mice compared to WT mice, whereas no significant reduction of LOXL2 was observed in the liver, LV, and RV (Figure S8A in the Data Supplement). We further studied the impact of skeletal muscle LOXL2 deficiency on PH-HFpEF by exposing WT and $Loxl2^{skm-/-}$ mice to HFD, which has been shown to reduce SIRT3 in skeletal muscle and lead to development of metabolic syndrome-associated PH-HFpEF.[13,22,61,62] Consistent with previous observations, HFD-exposed WT mice exhibited significantly higher body weight, glucose intolerance, pulmonary pressures, pulmonary vascular remodeling, LVEDP, and bi-ventricular hypertrophy than RD-exposed WT mice (Figure 7B–E and Figure S8B–D in the Data Supplement). Notably, female mice developed a very mild metabolic syndrome-associated PH-HFpEF phenotype (Figure S9 in the Data Supplement), which led us to focus on evaluation of the impact of skeletal muscle LOXL2 deficiency in male mice.

While no differences in body weight, LV hypertrophy, RV hypertrophy, LVEDP, and systolic blood pressures were observed, glucose intolerance, RVSP, and pulmonary vascular remodeling were significantly improved in HFD-exposed $Loxl2^{skm-/-}$ mice in comparison with WT mice fed with a HFD (Figure 7C–7E and S8B–E in the Data Supplement), suggesting a key role of skeletal muscle-secreted LOXL2 in regulating metabolic syndrome-associated PH-HFpEF. Additionally, higher circulating levels of LOXL2 were observed in plasma of HFD-exposed WT mice compared to RD-exposed mice (Figure S8F in the Data Supplement). Consistent with elevated LOXL2 levels, increased CNPY2 and decreased p53 levels were observed in $CD31^+$ endothelium and isolated PAECs of HFD-fed WT mice relative to RD-fed WT mice (Figure 7E and 7F and Figure S10 in the Data Supplement). Similarly, higher CNPY2 expression levels were also observed in α-SMA^+ layer and isolated PASMCs of HFD-fed WT mice (Figure 7E and 7G). While p53 expression was not significantly altered, expression levels of proliferating cell nuclear antigen (PCNA), which was up-regulated by CNPY2 overexpression, was increased in PASMCs of HFD-fed WT mice (Figure 7G and Figure S7E). Importantly, improved RVSP and pulmonary vascular remodeling were associated with reduced CNPY2 in PAECs and PASMCs of HFD-fed $Loxl2^{skm-/-}$ mice compared to WT animals (Figure 7E–G). Increased p53 levels and decreased PCNA levels in PAECs and PASMCs of HFD-fed $Loxl2^{skm-/-}$ mice, respectively, were also associated with improved RVSP and pulmonary vascular remodeling (Figure 7F and 7G and Figure S10 in the Data Supplement). These data indicate that LOXL2 may be an important endocrine signaling molecule which links skeletal muscle SIRT3

deficiency and remote CNPY2 regulation in the pulmonary vasculature. Furthermore, suppression of LOXL2 with pan-LOX(L) inhibitor, β-aminopropionitrile (BAPN, 100 mg/kg/day, drinking water), improved RVSP and RV hypertrophy, in relation to lower CNPY2 levels in PAECs and PASMCs, compared to mice fed with HFD alone (Figure S11 in the Data Supplement). Together, our data show that LOXL2 inhibition, either by skeletal muscle-specific knock-down or by pharmacological treatment, improves metabolic syndrome-associated PH-HFpEF, at least in part, by reducing CNPY2 in the pulmonary vasculature.

Discussion

In this study, we show that 1) there exists a systemic pathogenic impact of skeletal muscle SIRT3 deficiency in remote pulmonary vascular remodeling and PH-HFpEF; 2) decreased SIRT3 expression is associated with induction/secretion of LOXL2 in animal models and human subjects with PH-HFpEF; 3) CNPY2 is a key molecular target of skeletal muscle SIRT3 signaling in the pulmonary vasculature; 4) LOXL2 acts as an important endocrine signaling molecule linking skeletal muscle SIRT3 deficiency and remote CNPY2 regulation in the pulmonary vasculature (Figure 7H); and 5) absence of LOXL2 in skeletal muscle decreases CNPY2 expression, accompanied by reduced pulmonary vascular remodeling and lower pulmonary pressures. These findings not only provide new insights into the mechanistic basis of PH-HFpEF pathogenesis, but also lead to a broader understanding of how skeletal muscle defects affect pulmonary vascular health.

Global *Sirt3* knockout mice have been shown to develop spontaneous PH.[51] Several transcription factors critical to the development of PH, such as HIF1α, STAT3, and nuclear factor of activated T cells 2 (NFTAc2), have been found to be activated and present at elevated levels in PASMCs of SIRT3-deficient mice. Loss of function single nucleotide polymorphism (SNP) in *Sirt3* - rs1 1246020 has also been associated with metabolic syndrome and idiopathic PAH in humans.[31,63] Additionally, decreased SIRT3 in skeletal muscle has been associated with the development of diabetes, while caloric restriction- and exercise-induced increase in skeletal muscle SIRT3 brought multiple health benefits within the cardiovascular and the musculoskeletal system.[64] Exercise training has also been shown to improve exercise capacity and quality of life in patients with metabolic syndrome, PAH, and HFpEF,[64–66] highlighting the functional significance of SIRT3 activation in cardiopulmonary vascular health. The systemic impact of skeletal muscle SIRT3 deficiency on impaired glucose tolerance, pulmonary vascular remodeling, PH, and HFpEF observed in this study further provides support for this interconnection. Furthermore, the observation that PH-HFpHF patients exhibited lower skeletal muscle SIRT3 levels than those with HFpEF alone is of interest. Whether or not skeletal muscle SIRT3 deficiency is the key mechanism for disproportionate pathological pulmonary vascular remodeling in HFpEF needs to be further examined.

Skeletal muscle is increasingly recognized as an endocrine organ, which can produce and secrete hundreds of myokines to mediate communication between muscle and other organs, exerting their effects on glucose and lipid metabolism, endothelial function, tumor growth, bone formation, hypertrophy, appetite and etc.[67] Mitochondria, too,

communicate with other organelles within the cell and distant tissues through mitochondrial-derived peptides, mitokines, when experiencing mitochondrial stress.[68] As a critical regulator of mitochondrial function and integrity, SIRT3 loss of function may stress the mitochondria and induce the mitochondrial stress response (MSR), leading to the release of mitokines.[68,69] Using secretome analysis, we identified several myokines and/or myo-mitokines which can be regulated by SIRT3 in skeletal muscle. LOXL2 has been implicated in the development of several diseases, including lung fibrosis, liver fibrosis, cancer, PAH, and heart failure.[43,45,49] In PAH, increased LOXL2 expression is found in adventitial fibroblasts and is up-regulated by HIF1α, which is negatively regulated by SIRT3.[31,45,70] In heart failure, cardiac stress has been reported to induce production and secretion of LOXL2 in fibroblasts to trigger interstitial fibrosis through promotion of transforming growth factor-β (TGF-β) signaling, which can also be regulated by SIRT3 deficiency through hyperacetylation of glycogen synthase kinase 3β (GSK3β).[43,71] As we did not evaluate expressions and/or actions of LOXL2 in all cardiopulmonary cell types, it remains uncertain whether it originates from skeletal muscle or is regulated by other unknown mechanisms directly in the cardiopulmonary vasculature. Nevertheless, our data show that protein abundance levels of LOXL2 are not changed in PASMCs of Ob-Su rats and that CNPY2 levels in PAECs and PASMCs are modulated by skeletal muscle-specific deletion of LOXL2, further supporting the idea that skeletal muscle-secreted LOXL2 has a role in this context. Aside from its impact in the pulmonary vasculature, it is possible that elevated skeletal muscle and circulating levels of LOXL2 can promote structural and functional changes in the liver, lung, and heart, which may also contribute to the progression of the disease.

CNPY2 has been reported to possess a broad range of functions, including promotion of cell migration and proliferation, enhancement of angiogenesis, initiation of the PERK-CHOP pathway, and regulation of neurite outgrowth.[54,72–74] We showed herein that CNPY2 levels are increased in PAECs and PASMCs of two preclinical models of PH-HFpEF. Although we do not have PAECs and/or PASMCs from patients with PH-HFpEF, we observed similar increases in CNPY2 expression in PASMCs isolated from obese subjects. These results suggest that pathophysiological processes of metabolic syndrome and skeletal muscle SIRT3 deficiency may be associated with increased CNPY2 expression in the pulmonary vasculature. Previous study has demonstrated the role of CNPY2 in degradation of p53 in tumorigenesis.[58] In this study, we provide evidence that elevated CNPY2 down-regulates p53 in PAECs and PASMCs. We demonstrated that LOXL2 treatment, accompanied by increased CNPY2 and decreased p53, promotes PAECs migration/proliferation and PASMCs proliferation. Silencing of CNPY2 and overexpression of p53 rescue the migration and proliferation phenotypes induced by LOXL2 in PAECs and PASMCs. All of these support the idea that CNPY2 plays a critical role in facilitating LOXL2-mediated pulmonary vascular remodeling, in part through reduction of p53. Loss of p53 has been found in PAECs of patients with PAH.[59] Reduced p53 has also been shown to induce spontaneous PH, exaggerate monocrotaline-induced PH, and aggravate hypoxia-induced PH in various knockout murine models.[60,75–77] While endothelial cell-specific p53 knockout exaggerated PH, no aggravation of hypoxia-induced PH was observed in smooth muscle cell-specific p53 knockout,[59,78] suggesting an important vasculoprotective role of endothelial p53 in the

lung. In our study, increased p53 in PAECs, but not in PASMC, is associated with improved pulmonary vascular remodeling and reduced pulmonary pressures in HFD-fed *Loxl2*$^{skm-/-}$ mice. Our data may support the vasculoprotective role of endothelial p53, but it would be interesting to investigate this in future studies with human samples.

While secreted CNPY2 has been found in culture medium of hypoxia-exposed smooth muscle cells and in plasma of colorectal cancer patients,[73,79] CNPY2 was not detected in our skeletal muscle secretome analysis. Moreover, no change of CNPY2 levels was observed in circulation of rats with PH-HFpEF (Figure S12 in the Data Supplement). These data further suggest the existence of PAECs/PASMCs CNPY2 regulation signaling molecule(s) in skeletal muscle secretome. It remains unknown how LOXL2 elevates CNPY2 in PAECs and PASMCs. Altered CNPY2 expression has been attributed to HIF1α stabilization, CHOP upregulation, and microRNAs (miRNAs).[54,73,80] LOXL2 has been recently reported to stabilize HIF1α through inhibition of its prolyl hydroxylase (PHD)-dependent hydroxylation and to enhance aerobic glycolysis.[81] Additionally, LOXL2 has been shown to promote tumor progression via activation of IRE1-XBP1, which upregulates CHOP.[82] Further experiments are required to better understand the mechanism(s) in this context.

Despite a well-recognized female prevalence of PH, HFpEF, and PH-HFpEF,[7,83,84] we show that HFD-exposed female mice develop minimal progression of PH, bi-ventricular hypertrophy, and elevated LV filling pressure compared to their male counterparts. While this observation is in contrast to the common belief, our findings are consistent with previous reports that female mice are protective in experimental models of PH and HFpEF.[84,85] As ovariectomy exacerbates PH, but not HFpEF,[84,85] a number of other sex-modifiable factors beyond sex hormones, such as steroid hormones, immune and inflammatory responses, aging, mitochondrial function, and fatty acid metabolism, may be considered for future development of experimental models to integrate epidemiologic sex differences noted in PH-HFpEF.

Current treatments of PH-HFpEF that have focused on NO and ET-1 pathways have been shown to be ineffective or even harmful.[7,86] While sodium glucose cotransporter 2 (SGLT2) inhibitors have recently been reported to reduce pulmonary pressures in Ob-Su rats during exercise and in patients with heart failure,[23,87] the search for effective therapies for PH-HFpEF remains. Our findings that reduced skeletal muscle LOXL2 improves glucose intolerance and PH-HFpEF phenotype raise the possibility of LOXL2 targeting therapy for the treatment of PH-HFpEF. As pan-LOX(L) inhibitor, BAPN, has been shown to improve PAH, insulin sensitivity, and glucose uptake,[45,88,89] we evaluated the effect of BAPN in HFD-mouse and Ob-Su rat models of PH-HFpEF. Our data showed that BAPN treatment reduced pulmonary pressures and RV hypertrophy in association with decreased PAECs and PASMCs expression of CNPY2 in mice exposed to HFD (Figure S11 in the Data Supplement). BAPN treatment also improved fasting blood glucose and HbA1c levels in Ob-Su rats, but failed to improve RVSP and bi-ventricular hypertrophy in this more severe model of PH-HFpEF (Figure S13 in the Data Supplement). We noted that circulating concentration of LOXL2 is approximately 2.5 ng/ml in Ob-Su rats (Figure 3E), in contrast to 250 pg/ml in HFD-exposed mice (Figure S8F in the Data Supplement). This difference may explain, at least in part, a modest efficacy of BAPN, especially on pulmonary pressures, in

Ob-Su rats. These findings may suggest potential strategies aiming at reduction of skeletal muscle LOXL2 secretion and/or evaluation of small molecule inhibitors of LOXL2, such as PAT-1251, which has more than 400-fold selectivity over LOX (compared to the 6.6-fold selectivity of BAPN).[90] Interestingly, Ob-Su rats treated with nitrite and metformin, drugs which improve hyperglycemia and normalize pulmonary pressures via activation of SIRT3 in skeletal muscle,[11] exhibited lower circulating LOXL2 levels in comparison with untreated animals (Figure S14 in the Data Supplement). It is possible that skeletal muscle SIRT3 activated by nitrite and metformin reduces the induction/secretion of LOXL2, which in turn, maintains low expression level of CNPY2 in the pulmonary vasculature. The effect of metformin is currently under investigation in clinical trials in patients with PH-HFpEF. It would be interesting to examine whether LOXL2 levels are affected by metformin and its association with patient outcomes. While more studies are needed, this observation further supports the idea that reduced circulating LOXL2 levels may be a viable strategy for the treatment of PH-HFpEF. Our findings may also open a new avenue for approaches which would involve targeting CNPY2 in the management of PH-HFpEF.

In conclusion, our studies have uncovered several processes by which skeletal muscle SIRT3 deficiency can affect pulmonary vascular health in PH-HFpEF. Our findings also provide new insights into the mechanistic basis of the skeletal muscle-lung communication and identify skeletal muscle SIRT3, myokine LOXL2, and CNPY2 in the pulmonary vasculature as potential molecular targets for the development of therapeutic treatments in PH-HFpEF.

Limitations

Several potential limitations are acknowledged in the present studies: 1) lack of PAECs, PASMCs, and/or lung biopsies from patients with PH-HFpEF to assess the clinical relevance of PAECs and PASMCs expression of CNPY2 in human disease; 2) secretome analysis was performed in C2C12 myotubes, but not in human cells; 3) no obese controls for animal models; and 4) we were unable to evaluate the contribution of LOXL2 to PH-HFpEF in female mice due to their mild metabolic syndrome-associated PH-HFpEF phenotype.

Supplementary Material

Refer to Web version on PubMed Central for supplementary material.

Acknowledgments

The authors thank Dr. Sergei Snovida for helpful comments on the manuscript. The authors are grateful to Academia Sinica Common Mass Spectrometry Facilities for Proteomics and Protein Modification Analysis and Children's Hospital of Pittsburgh Rangos Research Center Animal Imaging Core. The authors also thank Dr. Amparo Cano, Dr. Yijen L. Wu, Dr. Shinya Tane, Dr. Andrea Frump, Dr. Yuan-Siao Chen, Tara S. Stakich, Gunner Halliday, Longfei Wang, Nathan Salamacha, Andrea Sebastiani, Scott Hahn, and Jordan Bullock for technical assistance and Elfy Chiang for production of the illustrations.

Sources of Funding

The research was supported by NIH/NHLBI R01HL142638 and American Heart Association 17SDG33400233 to Y-C. L., NIH/NHLBI 5P01HL103455 to M. T. G., in part by NIH/NHLBI R01HL113178, R01HL172488, and R01HL130261 to E. A. G., NIH/NHLBI R01HL127342, R01HL111656 and R01HL158108 to R. F. M, American Heart Association 23CDA1052251 to J-R. J., and NIH/NIA R01AG058659 to M. A. S.

References

1. Oktay AA, Rich JD, Shah SJ. The emerging epidemic of heart failure with preserved ejection fraction. Current heart failure reports. 2013;10:401–410. doi: 10.1007/s11897-013-0155-7 [PubMed: 24078336]
2. Lloyd-Jones D, Adams R, Carnethon M, De Simone G, Ferguson TB, Flegal K, Ford E, Furie K, Go A, Greenlund K, et al. Heart disease and stroke statistics−-2009 update: a report from the American Heart Association Statistics Committee and Stroke Statistics Subcommittee. Circulation. 2009;119:e21–181. doi: 10.1161/CIRCULATIONAHA.108.191261 [PubMed: 19075105]
3. Thenappan T, Shah SJ, Gomberg-Maitland M, Collander B, Vallakati A, Shroff P, Rich S. Clinical characteristics of pulmonary hypertension in patients with heart failure and preserved ejection fraction. Circ Heart Fail. 2011;4:257–265. doi: 10.1161/CIRCHEARTFAILURE.110.958801 [PubMed: 21411741]
4. Klapholz M, Maurer M, Lowe AM, Messineo F, Meisner JS, Mitchell J, Kalman J, Phillips RA, Steingart R, Brown EJ, Jr., et al. Hospitalization for heart failure in the presence of a normal left ventricular ejection fraction: results of the New York Heart Failure Registry. Journal of the American College of Cardiology. 2004;43:1432–1438. doi: 10.1016/j.jacc.2003.11.040 [PubMed: 15093880]
5. Simon MA, Vanderpool RR, Nouraie M, Bachman TN, White PM, Sugahara M, Gorcsan J, Parsley EL, Gladwin MT. Acute hemodynamic effects of inhaled sodium nitrite in pulmonary hypertension associated with heart failure with preserved ejection fraction. JCI Insight. 2016;1:e89620. doi: 10.1172/jci.insight.89620 [PubMed: 27812547]
6. Heidenreich PA, Albert NM, Allen LA, Bluemke DA, Butler J, Fonarow GC, Ikonomidis JS, Khavjou O, Konstam MA, Maddox TM, et al. Forecasting the impact of heart failure in the United States: a policy statement from the American Heart Association. Circ Heart Fail. 2013;6:606–619. doi: 10.1161/HHF.0b013e318291329a [PubMed: 23616602]
7. Brittain EL, Thenappan T, Huston JH, Agrawal V, Lai YC, Dixon D, Ryan JJ, Lewis EF, Redfield MM, Shah SJ, et al. Elucidating the Clinical Implications and Pathophysiology of Pulmonary Hypertension in Heart Failure With Preserved Ejection Fraction: A Call to Action: A Science Advisory From the American Heart Association. Circulation. 2022;146:e73–e88. doi: 10.1161/CIR.0000000000001079 [PubMed: 35862198]
8. Guazzi M Pulmonary hypertension in heart failure preserved ejection fraction: prevalence, pathophysiology, and clinical perspectives. Circ Heart Fail. 2014;7:367–377. doi: 10.1161/CIRCHEARTFAILURE.113.000823 [PubMed: 24643889]
9. Shapiro BP, McGoon MD, Redfield MM. Unexplained pulmonary hypertension in elderly patients. Chest. 2007;131:94–100. doi: 10.1378/chest.06-1571 [PubMed: 17218561]
10. Guazzi M, Borlaug BA. Pulmonary hypertension due to left heart disease. Circulation. 2012;126:975–990. doi: 10.1161/CIRCULATIONAHA.111.085761 [PubMed: 22908015]
11. Lai YC, Tabima DM, Dube JJ, Hughan KS, Vanderpool RR, Goncharov DA, St Croix CM, Garcia-Ocana A, Goncharova EA, Tofovic SP, et al. SIRT3-AMP-Activated Protein Kinase Activation by Nitrite and Metformin Improves Hyperglycemia and Normalizes Pulmonary Hypertension Associated With Heart Failure With Preserved Ejection Fraction. Circulation. 2016;133:717–731. doi: 10.1161/CIRCULATIONAHA.115.018935 [PubMed: 26813102]
12. Kelly NJ, Radder JE, Baust JJ, Burton CL, Lai YC, Potoka KC, Agostini BA, Wood JP, Bachman TN, Vanderpool RR, et al. Mouse Genome-Wide Association Study of Preclinical Group II Pulmonary Hypertension Identifies Epidermal Growth Factor Receptor. Am J Respir Cell Mol Biol. 2017;56:488–496. doi: 10.1165/rcmb.2016-0176OC [PubMed: 28085498]
13. Meng Q, Lai YC, Kelly NJ, Bueno M, Baust JJ, Bachman TN, Goncharov D, Vanderpool RR, Radder JE, Hu J, et al. Development of a Mouse Model of Metabolic Syndrome, Pulmonary Hypertension, and Heart Failure with Preserved Ejection Fraction. Am J Respir Cell Mol Biol. 2017;56:497–505. doi: 10.1165/rcmb.2016-0177OC [PubMed: 28118022]
14. Ranchoux B, Nadeau V, Bourgeois A, Provencher S, Tremblay E, Omura J, Cote N, Abu-Alhayja'a R, Dumais V, Nachbar RT, et al. Metabolic Syndrome Exacerbates Pulmonary Hypertension due to Left Heart Disease. Circ Res. 2019;125:449–466. doi: 10.1161/CIRCRESAHA.118.314555 [PubMed: 31154939]

15. Agrawal V, Fortune N, Yu S, Fuentes J, Shi F, Nichols D, Gleaves L, Poovey E, Wang TJ, Brittain EL, et al. Natriuretic peptide receptor C contributes to disproportionate right ventricular hypertrophy in a rodent model of obesity-induced heart failure with preserved ejection fraction with pulmonary hypertension. Pulm Circ. 2019;9:2045894019878599. doi: 10.1177/2045894019895452
16. Brittain EL, Talati M, Fortune N, Agrawal V, Meoli DF, West J, Hemnes AR. Adverse physiologic effects of Western diet on right ventricular structure and function: role of lipid accumulation and metabolic therapy. Pulm Circ. 2019;9:2045894018817741. doi: 10.1177/2045894018817741 [PubMed: 30451070]
17. Nguyen QL, Wang Y, Helbling N, Simon MA, Shiva S. Alterations in platelet bioenergetics in Group 2 PH-HFpEF patients. PLoS One. 2019;14:e0220490. doi: 10.1371/journal.pone.0220490 [PubMed: 31365585]
18. Agrawal V, Kropski JA, Gokey JJ, Kobeck E, Murphy MB, Murray KT, Fortune NL, Moore CS, Meoli DF, Monahan K, et al. Myeloid Cell Derived IL1beta Contributes to Pulmonary Hypertension in HFpEF. Circ Res. 2023;133:885–898. doi: 10.1161/CIRCRESAHA.123.323119 [PubMed: 37929582]
19. Meoli DF, Su YR, Brittain EL, Robbins IM, Hemnes AR, Monahan K. The transpulmonary ratio of endothelin 1 is elevated in patients with preserved left ventricular ejection fraction and combined pre- and post-capillary pulmonary hypertension. Pulm Circ. 2018;8:2045893217745019. doi: 10.1177/2045893217745019 [PubMed: 29251543]
20. Chowdhury MA, Moukarbel GV, Gupta R, Frank SM, Anderson AM, Liu LC, Khouri SJ. Endothelin 1 Is Associated with Heart Failure Hospitalization and Long-Term Mortality in Patients with Heart Failure with Preserved Ejection Fraction and Pulmonary Hypertension. Cardiology. 2019;143:124–133. doi: 10.1159/000501100 [PubMed: 31514181]
21. Obokata M, Kane GC, Reddy YNV, Melenovsky V, Olson TP, Jarolim P, Borlaug BA. The neurohormonal basis of pulmonary hypertension in heart failure with preserved ejection fraction. Eur Heart J. 2019;40:3707–3717. doi: 10.1093/eurheartj/ehz626 [PubMed: 31513270]
22. Hansmann G, Wagner RA, Schellong S, Perez VA, Urashima T, Wang L, Sheikh AY, Suen RS, Stewart DJ, Rabinovitch M. Pulmonary arterial hypertension is linked to insulin resistance and reversed by peroxisome proliferator-activated receptor-gamma activation. Circulation. 2007;115:1275–1284. doi: 10.1161/CIRCULATIONAHA.106.663120 [PubMed: 17339547]
23. Satoh T, Wang L, Espinosa-Diez C, Wang B, Hahn SA, Noda K, Rochon ER, Dent MR, Levine A, Baust JJ, et al. Metabolic Syndrome Mediates ROS-miR-193b-NFYA-Dependent Down Regulation of sGC and Contributes to Exercise-Induced Pulmonary Hypertension in HFpEF. Circulation. 2021;144:615–637. doi: 10.1161/CIRCULATIONAHA.121.053889 [PubMed: 34157861]
24. Shah SJ, Borlaug BA, Kitzman DW, McCulloch AD, Blaxall BC, Agarwal R, Chirinos JA, Collins S, Deo RC, Gladwin MT, et al. Research Priorities for Heart Failure With Preserved Ejection Fraction: National Heart, Lung, and Blood Institute Working Group Summary. Circulation. 2020;141:1001–1026. doi: 10.1161/CIRCULATIONAHA.119.041886 [PubMed: 32202936]
25. Guazzi M, Naeije R. Pulmonary Hypertension in Heart Failure: Pathophysiology, Pathobiology, and Emerging Clinical Perspectives. Journal of the American College of Cardiology. 2017;69:1718–1734. doi: 10.1016/j.jacc.2017.01.051 [PubMed: 28359519]
26. Lai YC, Wang L, Gladwin MT. Insights into the pulmonary vascular complications of heart failure with preserved ejection fraction. J Physiol. 2019;597:1143–1156. doi: 10.1113/JP275858 [PubMed: 30549058]
27. Shah SJ, Kitzman DW, Borlaug BA, van Heerebeek L, Zile MR, Kass DA, Paulus WJ. Phenotype-Specific Treatment of Heart Failure With Preserved Ejection Fraction: A Multiorgan Roadmap. Circulation. 2016;134:73–90. doi: 10.1161/CIRCULATIONAHA.116.021884 [PubMed: 27358439]
28. Zotter-Tufaro C, Mascherbauer J, Duca F, Koell B, Aschauer S, Kammerlander AA, Panzenboeck A, Sadushi-Kolici R, Bangert C, Laimer D, et al. Prognostic Significance and Determinants of the 6-Min Walk Test in Patients With Heart Failure and Preserved Ejection Fraction. JACC Heart failure. 2015;3:459–466. doi: 10.1016/j.jchf.2015.01.010 [PubMed: 26046839]

29. Kitzman DW, Nicklas B, Kraus WE, Lyles MF, Eggebeen J, Morgan TM, Haykowsky M. Skeletal muscle abnormalities and exercise intolerance in older patients with heart failure and preserved ejection fraction. Am J Physiol Heart Circ Physiol. 2014;306:H1364–1370. doi: 10.1152/ajpheart.00004.2014 [PubMed: 24658015]
30. Oktay AA, Shah SJ. Diagnosis and management of heart failure with preserved ejection fraction: 10 key lessons. Curr Cardiol Rev. 2015;11:42–52. doi: 10.2174/1573403×09666131117131217 [PubMed: 24251461]
31. Hirschey MD, Shimazu T, Jing E, Grueter CA, Collins AM, Aouizerat B, Stancakova A, Goetzman E, Lam MM, Schwer B, et al. SIRT3 deficiency and mitochondrial protein hyperacetylation accelerate the development of the metabolic syndrome. Mol Cell. 2011;44:177–190. doi: 10.1016/j.molcel.2011.07.019 [PubMed: 21856199]
32. Paulin R, Dromparis P, Sutendra G, Gurtu V, Zervopoulos S, Bowers L, Haromy A, Webster L, Provencher S, Bonnet S, et al. Sirtuin 3 deficiency is associated with inhibited mitochondrial function and pulmonary arterial hypertension in rodents and humans. Cell Metab. 2014;20:827–839. doi: 10.1016/j.cmet.2014.08.011 [PubMed: 25284742]
33. Bellizzi D, Rose G, Cavalcante P, Covello G, Dato S, De Rango F, Greco V, Maggiolini M, Feraco E, Mari V, et al. A novel VNTR enhancer within the SIRT3 gene, a human homologue of SIR2, is associated with survival at oldest ages. Genomics. 2005;85:258–263. doi: 10.1016/j.ygeno.2004.11.003 [PubMed: 15676284]
34. Uhl FE, Vierkotten S, Wagner DE, Burgstaller G, Costa R, Koch I, Lindner M, Meiners S, Eickelberg O, Konigshoff M. Preclinical validation and imaging of Wnt-induced repair in human 3D lung tissue cultures. Eur Respir J. 2015;46:1150–1166. doi: 10.1183/09031936.00183214 [PubMed: 25929950]
35. Fernandez-Marcos PJ, Jeninga EH, Canto C, Harach T, de Boer VC, Andreux P, Moullan N, Pirinen E, Yamamoto H, Houten SM, et al. Muscle or liver-specific Sirt3 deficiency induces hyperacetylation of mitochondrial proteins without affecting global metabolic homeostasis. Sci Rep. 2012;2:425. doi: 10.1038/srep00425 [PubMed: 22645641]
36. Martin A, Salvador F, Moreno-Bueno G, Floristan A, Ruiz-Herguido C, Cuevas EP, Morales S, Santos V, Csiszar K, Dubus P, et al. Lysyl oxidase-like 2 represses Notch1 expression in the skin to promote squamous cell carcinoma progression. EMBO J. 2015;34:1090–1109. doi: 10.15252/embj.201489975 [PubMed: 25759215]
37. Kim AJ, Francis R, Liu X, Devine WA, Ramirez R, Anderton SJ, Wong LY, Faruque F, Gabriel GC, Chung W, et al. Microcomputed tomography provides high accuracy congenital heart disease diagnosis in neonatal and fetal mice. Circ Cardiovasc Imaging. 2013;6:551–559. doi: 10.1161/CIRCIMAGING.113.000279 [PubMed: 23759365]
38. Goncharov DA, Kudryashova TV, Ziai H, Ihida-Stansbury K, DeLisser H, Krymskaya VP, Tuder RM, Kawut SM, Goncharova EA. Mammalian target of rapamycin complex 2 (mTORC2) coordinates pulmonary artery smooth muscle cell metabolism, proliferation, and survival in pulmonary arterial hypertension. Circulation. 2014;129:864–874. doi: 10.1161/CIRCULATIONAHA.113.004581 [PubMed: 24270265]
39. Bostrom P, Wu J, Jedrychowski MP, Korde A, Ye L, Lo JC, Rasbach KA, Bostrom EA, Choi JH, Long JZ, et al. A PGC1-alpha-dependent myokine that drives brown-fat-like development of white fat and thermogenesis. Nature. 2012;481:463–468. doi: 10.1038/nature10777 [PubMed: 22237023]
40. Kim KH, Jeong YT, Oh H, Kim SH, Cho JM, Kim YN, Kim SS, Kim DH, Hur KY, Kim HK, et al. Autophagy deficiency leads to protection from obesity and insulin resistance by inducing Fgf21 as a mitokine. Nat Med. 2013;19:83–92. doi: 10.1038/nm.3014 [PubMed: 23202295]
41. Chung HK, Ryu D, Kim KS, Chang JY, Kim YK, Yi HS, Kang SG, Choi MJ, Lee SE, Jung SB, et al. Growth differentiation factor 15 is a myomitokine governing systemic energy homeostasis. J Cell Biol. 2017;216:149–165. doi: 10.1083/jcb.201607110 [PubMed: 27986797]
42. Zhang L, Elias JE. Relative Protein Quantification Using Tandem Mass Tag Mass Spectrometry. Methods Mol Biol. 2017;1550:185–198. doi: 10.1007/978-1-4939-6747-6_14 [PubMed: 28188531]

43. Yang J, Savvatis K, Kang JS, Fan P, Zhong H, Schwartz K, Barry V, Mikels-Vigdal A, Karpinski S, Kornyeyev D, et al. Targeting LOXL2 for cardiac interstitial fibrosis and heart failure treatment. Nat Commun. 2016;7:13710. doi: 10.1038/ncomms13710 [PubMed: 27966531]
44. Cahill E, Costello CM, Rowan SC, Harkin S, Howell K, Leonard MO, Southwood M, Cummins EP, Fitzpatrick SF, Taylor CT, et al. Gremlin plays a key role in the pathogenesis of pulmonary hypertension. Circulation. 2012;125:920–930. doi: 10.1161/CIRCULATIONAHA.111.038125 [PubMed: 22247494]
45. Nave AH, Mizikova I, Niess G, Steenbock H, Reichenberger F, Talavera ML, Veit F, Herold S, Mayer K, Vadasz I, et al. Lysyl oxidases play a causal role in vascular remodeling in clinical and experimental pulmonary arterial hypertension. Arterioscler Thromb Vasc Biol. 2014;34:1446–1458. doi: 10.1161/ATVBAHA.114.303534 [PubMed: 24833797]
46. Li P, Oparil S, Feng W, Chen YF. Hypoxia-responsive growth factors upregulate periostin and osteopontin expression via distinct signaling pathways in rat pulmonary arterial smooth muscle cells. Journal of applied physiology. 2004;97:1550–1558; discussion 1549. doi: 10.1152/japplphysiol.01311.2003 [PubMed: 15121739]
47. Ciuclan L, Sheppard K, Dong L, Sutton D, Duggan N, Hussey M, Simmons J, Morrell NW, Jarai G, Edwards M, et al. Treatment with anti-gremlin 1 antibody ameliorates chronic hypoxia/SU5416-induced pulmonary arterial hypertension in mice. Am J Pathol. 2013;183:1461–1473. doi: 10.1016/j.ajpath.2013.07.017 [PubMed: 24160323]
48. Vadasz Z, Kessler O, Akiri G, Gengrinovitch S, Kagan HM, Baruch Y, Izhak OB, Neufeld G. Abnormal deposition of collagen around hepatocytes in Wilson's disease is associated with hepatocyte specific expression of lysyl oxidase and lysyl oxidase like protein-2. Journal of hepatology. 2005;43:499–507. doi: 10.1016/j.jhep.2005.02.052 [PubMed: 16023247]
49. Barry-Hamilton V, Spangler R, Marshall D, McCauley S, Rodriguez HM, Oyasu M, Mikels A, Vaysberg M, Ghermazien H, Wai C, et al. Allosteric inhibition of lysyl oxidase-like-2 impedes the development of a pathologic microenvironment. Nat Med. 2010;16:1009–1017. doi: 10.1038/nm.2208 [PubMed: 20818376]
50. Steppan J, Wang H, Bergman Y, Rauer MJ, Tan S, Jandu S, Nandakumar K, Barreto-Ortiz S, Cole RN, Boronina TN, et al. Lysyl oxidase-like 2 depletion is protective in age-associated vascular stiffening. Am J Physiol Heart Circ Physiol. 2019;317:H49–H59. doi: 10.1152/ajpheart.00670.2018 [PubMed: 31002285]
51. Cuevas EP, Eraso P, Mazon MJ, Santos V, Moreno-Bueno G, Cano A, Portillo F. LOXL2 drives epithelial-mesenchymal transition via activation of IRE1-XBP1 signalling pathway. Sci Rep. 2017;7:44988. doi: 10.1038/srep44988 [PubMed: 28332555]
52. Schiattarella GG, Altamirano F, Tong D, French KM, Villalobos E, Kim SY, Luo X, Jiang N, May HI, Wang ZV, et al. Nitrosative stress drives heart failure with preserved ejection fraction. Nature. 2019;568:351–356. doi: 10.1038/s41586-019-1100-z [PubMed: 30971818]
53. Akram KM, Yates LL, Mongey R, Rothery S, Gaboriau DCA, Sanderson J, Hind M, Griffiths M, Dean CH. Live imaging of alveologenesis in precision-cut lung slices reveals dynamic epithelial cell behaviour. Nat Commun. 2019;10:1178. doi: 10.1038/s41467-019-09067-3 [PubMed: 30862802]
54. Hong F, Liu B, Wu BX, Morreall J, Roth B, Davies C, Sun S, Diehl JA, Li Z. CNPY2 is a key initiator of the PERK-CHOP pathway of the unfolded protein response. Nat Struct Mol Biol. 2017;24:834–839. doi: 10.1038/nsmb.3458 [PubMed: 28869608]
55. Yeager ME, Reddy MB, Nguyen CM, Colvin KL, Ivy DD, Stenmark KR. Activation of the unfolded protein response is associated with pulmonary hypertension. Pulm Circ. 2012;2:229–240. doi: 10.4103/2045-8932.97613 [PubMed: 22837864]
56. Shimizu T, Higashijima Y, Kanki Y, Nakaki R, Kawamura T, Urade Y, Wada Y. PERK inhibition attenuates vascular remodeling in pulmonary arterial hypertension caused by BMPR2 mutation. Sci Signal. 2021;14:eabb3616. doi: 10.1126/scisignal.abb3616 [PubMed: 33500333]
57. Zhuan B, Wang X, Wang MD, Li ZC, Yuan Q, Xie J, Yang Z. Hypoxia induces pulmonary artery smooth muscle dysfunction through mitochondrial fragmentation-mediated endoplasmic reticulum stress. Aging (Albany NY). 2020;12:23684–23697. doi: 10.18632/aging.103892 [PubMed: 33221740]

58. Hong F, Lin CY, Yan J, Dong Y, Ouyang Y, Kim D, Zhang X, Liu B, Sun S, Gu W, et al. Canopy Homolog 2 contributes to liver oncogenesis by promoting unfolded protein response-dependent destabilization of tumor protein P53. Hepatology. 2022;76:1587–1601. doi: 10.1002/hep.32318 [PubMed: 34986508]
59. Bhagwani AR, Ali M, Piper B, Liu M, Hudson J, Kelly N, Bogamuwa S, Yang H, Londino JD, Bednash JS, et al. A p53-TLR3 axis ameliorates pulmonary hypertension by inducing BMPR2 via IRF3. iScience. 2023;26:105935. doi: 10.1016/j.isci.2023.105935 [PubMed: 36685041]
60. Jacquin S, Rincheval V, Mignotte B, Richard S, Humbert M, Mercier O, Londono-Vallejo A, Fadel E, Eddahibi S. Inactivation of p53 Is Sufficient to Induce Development of Pulmonary Hypertension in Rats. PLoS One. 2015;10:e0131940. doi: 10.1371/journal.pone.0131940 [PubMed: 26121334]
61. Kelley EE, Baust J, Bonacci G, Golin-Bisello F, Devlin JE, St Croix CM, Watkins SC, Gor S, Cantu-Medellin N, Weidert ER, et al. Fatty acid nitroalkenes ameliorate glucose intolerance and pulmonary hypertension in high-fat diet-induced obesity. Cardiovasc Res. 2014;101:352–363. doi: 10.1093/cvr/cvt341 [PubMed: 24385344]
62. Jing E, Emanuelli B, Hirschey MD, Boucher J, Lee KY, Lombard D, Verdin EM, Kahn CR. Sirtuin-3 (Sirt3) regulates skeletal muscle metabolism and insulin signaling via altered mitochondrial oxidation and reactive oxygen species production. Proc Natl Acad Sci U S A. 2011;108:14608–14613. doi: 10.1073/pnas.1111308108 [PubMed: 21873205]
63. Paulin R, Dromparis P, Sutendra G, Gurtu V, Zervopoulos S, Bowers L, Haromy A, Webster L, Provencher S, Bonnet S, et al. Sirtuin 3 deficiency is associated with inhibited mitochondrial function and pulmonary arterial hypertension in rodents and humans. Cell metabolism. 2014;20:827–839. doi: 10.1016/j.cmet.2014.08.011 [PubMed: 25284742]
64. Palacios OM, Carmona JJ, Michan S, Chen KY, Manabe Y, Ward JL, Goodyear LJ, Tong Q. Diet and exercise signals regulate SIRT3 and activate AMPK and PGC-1alpha in skeletal muscle. Aging (Albany NY). 2009;1:771–783. doi: 10.18632/aging.100075 [PubMed: 20157566]
65. Mereles D, Ehlken N, Kreuscher S, et al. Exercise and respiratory training improve exercise capacity and quality of life in patients with severe chronic pulmonary hypertension. Circulation. 2006;114:1482–1489. doi: 10.1161/CIRCULATIONAHA.106.618397 [PubMed: 16982941]
66. Pandey A, Parashar A, Kumbhani DJ, Agarwal S, Garg J, Kitzman D, Levine BD, Drazner M, Berry JD. Exercise training in patients with heart failure and preserved ejection fraction: meta-analysis of randomized control trials. Circ Heart Fail. 2015;8:33–40. doi: 10.1161/CIRCHEARTFAILURE.114.001615 [PubMed: 25399909]
67. Severinsen MCK, Pedersen BK. Muscle-Organ Crosstalk: The Emerging Roles of Myokines. Endocr Rev. 2020;41:594–609. doi: 10.1210/endrev/bnaa016 [PubMed: 32393961]
68. Mottis A, Herzig S, Auwerx J. Mitocellular communication: Shaping health and disease. Science. 2019;366:827–832. doi: 10.1126/science.aax3768 [PubMed: 31727828]
69. Papa L, Germain D. SirT3 regulates the mitochondrial unfolded protein response. Mol Cell Biol. 2014;34:699–710. doi: 10.1128/MCB.01337-13 [PubMed: 24324009]
70. Finley LW, Carracedo A, Lee J, Souza A, Egia A, Zhang J, Teruya-Feldstein J, Moreira PI, Cardoso SM, Clish CB, et al. SIRT3 opposes reprogramming of cancer cell metabolism through HIF1alpha destabilization. Cancer Cell. 2011;19:416–428. doi: 10.1016/j.ccr.2011.02.014 [PubMed: 21397863]
71. Sundaresan NR, Bindu S, Pillai VB, Samant S, Pan Y, Huang JY, Gupta M, Nagalingam RS, Wolfgeher D, Verdin E, et al. SIRT3 Blocks Aging-Associated Tissue Fibrosis in Mice by Deacetylating and Activating Glycogen Synthase Kinase 3beta. Mol Cell Biol. 2015;36:678–692. doi: 10.1128/MCB.00586-15 [PubMed: 26667039]
72. Wang D, Wang ZM, Zhang S, Wu HJ, Tao YM. Canopy Homolog 2 Expression Predicts Poor Prognosis in Hepatocellular Carcinoma with Tumor Hemorrhage. Cell Physiol Biochem. 2018;50:2017–2028. doi: 10.1159/000495048 [PubMed: 30415246]
73. Guo J, Zhang Y, Mihic A, Li SH, Sun Z, Shao Z, Wu J, Weisel RD, Li RK. A secreted protein (Canopy 2, CNPY2) enhances angiogenesis and promotes smooth muscle cell migration and proliferation. Cardiovasc Res. 2015;105:383–393. doi: 10.1093/cvr/cvv010 [PubMed: 25589425]

74. Bornhauser BC, Olsson PA, Lindholm D. MSAP is a novel MIR-interacting protein that enhances neurite outgrowth and increases myosin regulatory light chain. J Biol Chem. 2003;278:35412–35420. doi: 10.1074/jbc.M306271200 [PubMed: 12826659]

75. Mizuno S, Bogaard HJ, Kraskauskas D, Alhussaini A, Gomez-Arroyo J, Voelkel NF, Ishizaki T. p53 Gene deficiency promotes hypoxia-induced pulmonary hypertension and vascular remodeling in mice. Am J Physiol Lung Cell Mol Physiol. 2011;300:L753–761. doi: 10.1152/ajplung.00286.2010 [PubMed: 21335523]

76. Mouraret N, Marcos E, Abid S, Gary-Bobo G, Saker M, Houssaini A, Dubois-Rande JL, Boyer L, Boczkowski J, Derumeaux G, et al. Activation of lung p53 by Nutlin-3a prevents and reverses experimental pulmonary hypertension. Circulation. 2013;127:1664–1676. doi: 10.1161/CIRCULATIONAHA.113.002434 [PubMed: 23513067]

77. Hennigs JK, Cao A, Li CG, Shi M, Mienert J, Miyagawa K, Korbelin J, Marciano DP, Chen PI, Roughley M, et al. PPARgamma-p53-Mediated Vasculoregenerative Program to Reverse Pulmonary Hypertension. Circ Res. 2021;128:401–418. doi: 10.1161/CIRCRESAHA.119.316339 [PubMed: 33322916]

78. Wakasugi T, Shimizu I, Yoshida Y, Hayashi Y, Ikegami R, Suda M, Katsuumi G, Nakao M, Hoyano M, Kashimura T, et al. Role of smooth muscle cell p53 in pulmonary arterial hypertension. PLoS One. 2019;14:e0212889. doi: 10.1371/journal.pone.0212889 [PubMed: 30807606]

79. Yan P, Gong H, Zhai X, Feng Y, Wu J, He S, Guo J, Wang X, Guo R, Xie J, et al. Decreasing CNPY2 Expression Diminishes Colorectal Tumor Growth and Development through Activation of p53 Pathway. Am J Pathol. 2016;186:1015–1024. doi: 10.1016/j.ajpath.2015.11.012 [PubMed: 26835537]

80. Wang H, Kanmangne D, Li R, Qian Z, Xia X, Wang X, Wang T. miR−30a−3p suppresses the proliferation and migration of lung adenocarcinoma cells by downregulating CNPY2. Oncol Rep. 2020;43:646–654. doi: 10.3892/or.2019.7423 [PubMed: 31894275]

81. Li R, Li H, Zhu L, Zhang X, Liu D, Li Q, Ni B, Hu L, Zhang Z, Zhang Y, et al. Reciprocal regulation of LOXL2 and HIF1alpha drives the Warburg effect to support pancreatic cancer aggressiveness. Cell Death Dis. 2021;12:1106. doi: 10.1038/s41419-021-04391-3 [PubMed: 34836938]

82. Hu H, Tian M, Ding C, Yu S. The C/EBP Homologous Protein (CHOP) Transcription Factor Functions in Endoplasmic Reticulum Stress-Induced Apoptosis and Microbial Infection. Front Immunol. 2018;9:3083. doi: 10.3389/fimmu.2018.03083 [PubMed: 30662442]

83. Sotomi Y, Hikoso S, Nakatani D, Mizuno H, Okada K, Dohi T, Kitamura T, Sunaga A, Kida H, Oeun B, et al. Sex Differences in Heart Failure With Preserved Ejection Fraction. J Am Heart Assoc. 2021;10:e018574. doi: 10.1161/JAHA.120.018574 [PubMed: 33619973]

84. Hester J, Ventetuolo C, Lahm T. Sex, Gender, and Sex Hormones in Pulmonary Hypertension and Right Ventricular Failure. Compr Physiol. 2019;10:125–170. doi: 10.1002/cphy.c190011 [PubMed: 31853950]

85. Tong D, Schiattarella GG, Jiang N, May HI, Lavandero S, Gillette TG, Hill JA. Female Sex Is Protective in a Preclinical Model of Heart Failure With Preserved Ejection Fraction. Circulation. 2019;140:1769–1771. doi: 10.1161/CIRCULATIONAHA.119.042267 [PubMed: 31738599]

86. Cheli M, Vachiery JL. Controversies in pulmonary hypertension due to left heart disease. F1000Prime Rep. 2015;7:07. doi: 10.12703/P7-07 [PubMed: 25705390]

87. Nassif ME, Qintar M, Windsor SL, Jermyn R, Shavelle DM, Tang F, Lamba S, Bhatt K, Brush J, Civitello A, et al. Empagliflozin Effects on Pulmonary Artery Pressure in Patients With Heart Failure: Results From the EMBRACE-HF Trial. Circulation. 2021;143:1673–1686. doi: 10.1161/CIRCULATIONAHA.120.052503 [PubMed: 33550815]

88. Miana M, Galan M, Martinez-Martinez E, Varona S, Jurado-Lopez R, Bausa-Miranda B, Antequera A, Luaces M, Martinez-Gonzalez J, Rodriguez C, et al. The lysyl oxidase inhibitor beta-aminopropionitrile reduces body weight gain and improves the metabolic profile in diet-induced obesity in rats. Dis Model Mech. 2015;8:543–551. doi: 10.1242/dmm.020107 [PubMed: 26035864]

89. Bertero T, Oldham WM, Cottrill KA, Pisano S, Vanderpool RR, Yu Q, Zhao J, Tai Y, Tang Y, Zhang YY, et al. Vascular stiffness mechanoactivates YAP/TAZ-dependent glutaminolysis to drive

pulmonary hypertension. J Clin Invest. 2016;126:3313–3335. doi: 10.1172/JCI86387 [PubMed: 27548520]

90. Hutchinson JH, Rowbottom MW, Lonergan D, Darlington J, Prodanovich P, King CD, Evans JF, Bain G. Small Molecule Lysyl Oxidase-like 2 (LOXL2) Inhibitors: The Identification of an Inhibitor Selective for LOXL2 over LOX. ACS Med Chem Lett. 2017;8:423–427. doi: 10.1021/acsmedchemlett.7b00014 [PubMed: 28435530]

Clinical Perspective

What Is New?

- This study describes a systemic pathogenic impact of skeletal muscle sirtuin-3 (SIRT3) deficiency in remote pulmonary vascular remodeling and PH-HFpEF.
- Lysyl oxidase homolog 2 (LOXL2) acts as an important endocrine signaling molecule linking skeletal muscle SIRT3 deficiency and remote canopy fibroblast growth factor signaling regulator 2 (CNPY2) regulation in the pulmonary vasculature.

What Are the Clinical Implications?

- These findings provide a broader understanding of how skeletal muscle defects, which are associated with severe exercise intolerance and worsening functional capacity in patients with PH-HFpEF, affect pulmonary vascular health.
- This study identifies skeletal muscle SIRT3, myokine LOXL2, and CNPY2 in the pulmonary vasculature as potential molecular targets for the development of therapeutic treatments in PH-HFpEF.

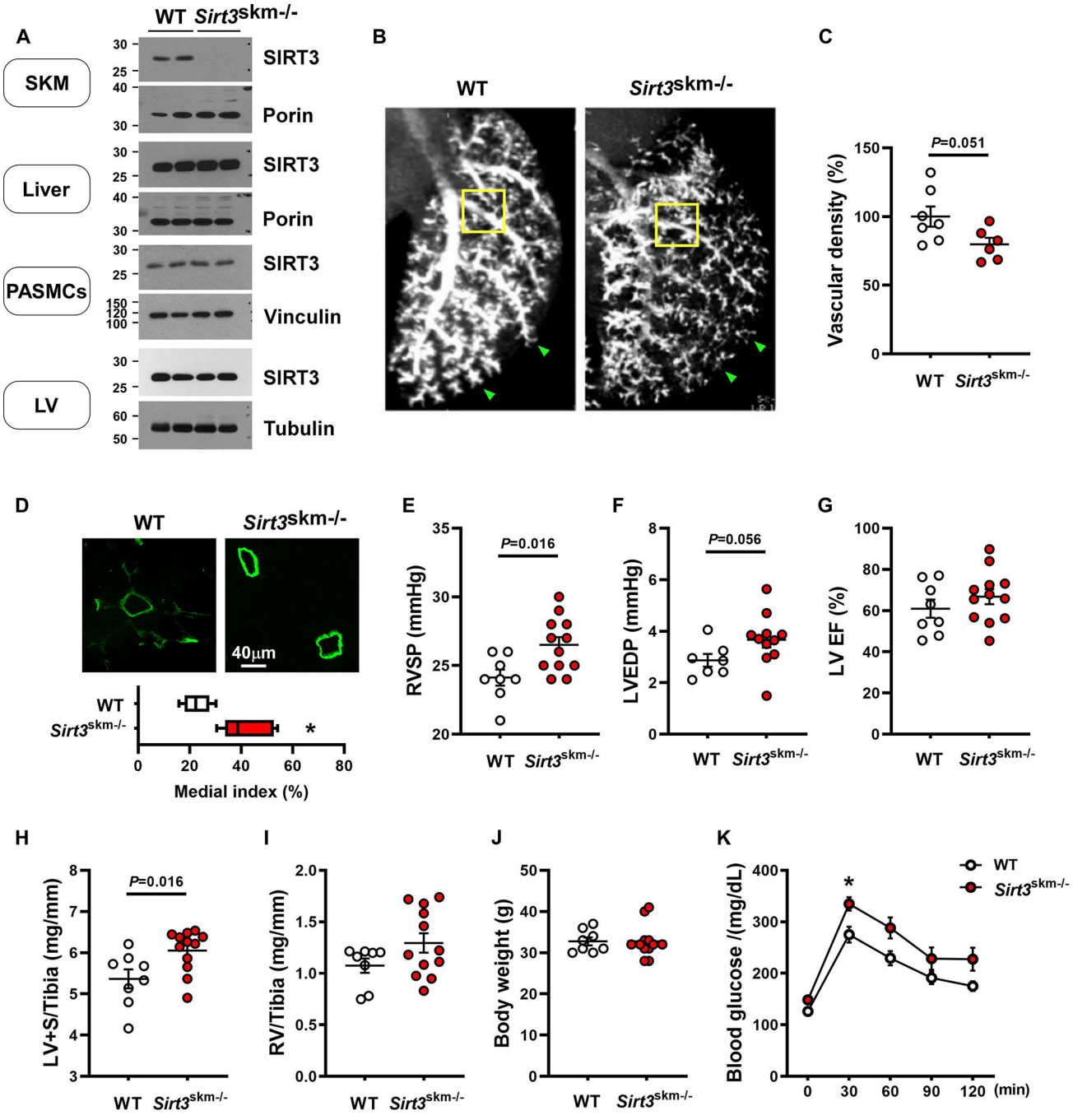

Figure 1.

Absence of SIRT3 in skeletal muscle leads to reduced pulmonary vascular density, increased pulmonary vascular remodeling, and elevated pulmonary pressures. **A**, SIRT3 protein levels in soleus, liver, pulmonary artery smooth muscle cells (PASMCs), and left ventricle (LV) of WT and *Sirt3*$^{skm-/-}$ mice. **B**, Representative micro-CT images of lungs infused with Mercox II resin from WT and *Sirt3*$^{skm-/-}$ mice. Reduction in vascular density, with narrowed vascular diameter (yellow square), and decreased peripheral vasculature (green arrowheads), was observed in *Sirt3*$^{skm-/-}$ mice. **C**, Volumetric analysis of the pulmonary vasculature. **D**,

Representative images of lung sections stained with α-smooth muscle actin (α-SMA, 20X). **E-G**, Right ventricular systolic pressure (RVSP; **E**), left ventricular end-diastolic pressure (LVEDP; **F**), and LV ejection fraction (LVEF, **G**) were measured in WT and *Sirt3*$^{\text{km}-/-}$ mice. **H** and **I**, LV and RV mass normalized to tibial length. **J-K**, Body weight (**J**) and glucose tolerant abilities (**K**) were measured. All mice were fed on regular diet starting at age of 8 weeks for 16 weeks. Data are mean ± SEM; n = 6–12 mice/group. Statistical comparisons were performed using Mann-Whitney U-test. For Figure 1K, two-way ANOVA followed by Bonferroni's *post hoc* test was performed. $*P < 0.05$.

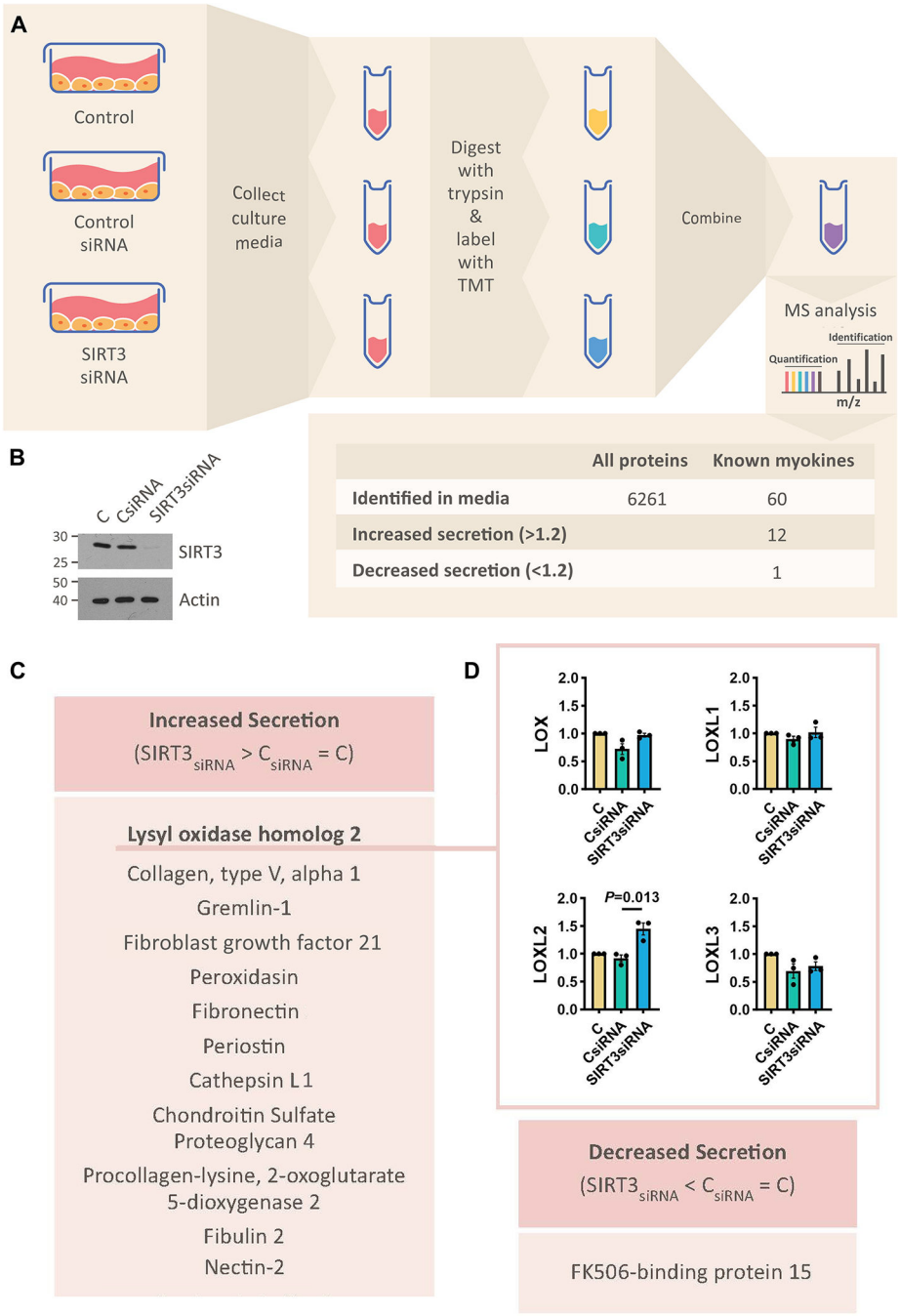

Figure 2.

Secreted proteins associated with skeletal muscle SIRT3 deficiency identified by mass spectrometry. **A**, Schematic overview of comparative secretome analysis. Briefly, each sample (condition/replicate) was labeled with a unique TMT reagent tag at the peptide level. While these tags are isobaric, they are different with respect to the position of isotopically heavy nuclei in their structural backbone. After labeling, the individual samples are combined to produce a single multiplexed sample. Upon fragmentation in the mass spectrometer, a sample-specific fragment, a reporter ion, is released and recorded in the

mass spectrum. Labeled peptides derived from different samples will have a unique reporter ion whose abundance is related to the abundance of the peptide in the given sample. Relative quantification is performed by measuring the relative abundances of the reporter ions released during fragmentation of “protein-specific” tryptic peptides. **B**, Efficiency of siRNA-mediated knock-down of SIRT3 in C2C12 myotubes. **C**, Proteins identified as differentially regulated by SIRT3. **D**, Abundance ratio of lysyl oxidases (LOX) and LOX-like family members (LOXL1, LOXL2 and LOXL3) for 3 conditions (with 3 biological replicates each). Data are mean ± SEM. Comparisons of parameters were performed using unpaired Student’s *t*-test after testing for normality with Shapiro-Wilk test.

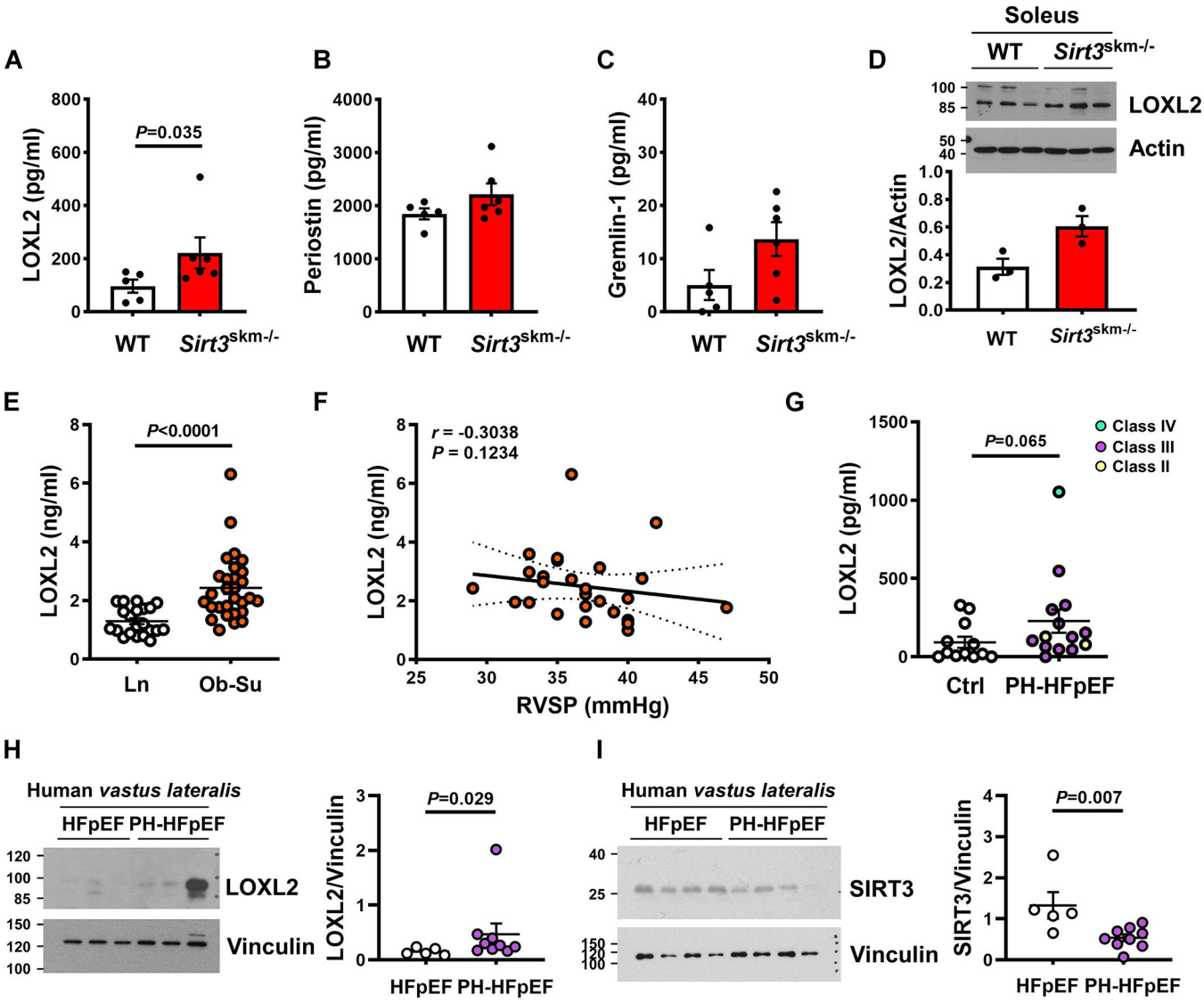

Figure 3.

Increased LOXL2 in plasma and skeletal muscle of *Sirt3*$^{skm-/-}$ mice, Ob-Su rats and patients with PH-HFpEF. Plasma levels of LOXL2 (**A**), periostin (**B**), and Grem1 (**C**) were measured in WT and *Sirt3*$^{skm-/-}$ mice. **D**, Representative Western blots for LOXL2 protein expression levels in soleus of *Sirt3*$^{skm-/-}$ and WT mice. **E**, Plasma levels of LOXL2 were measured in Ob-Su rat model of PH-HFpEF. **F**, Correlation between RVSP and LOXL2 in Ob-Su rats. Spearman *r* is shown. **G**, Circulating levels of LOXL2 were measured in plasma of control subjects ($n = 12$) and patients with PH-HFpEF [$n = 14$; Age: 70.4 ± 7.9; male gender: 8; BMI: 37.2 ± 10.2; mPAP: 39.9 ± 8.6 mmHg; PCWP: 20 ± 7.8 mmHg; WHO function class II: 2 (14%), III: 11 (79%), and IV: 1 (7%)]. **H** and **I**, Representative Western blots of LOXL2 (**H**) and SIRT3 (**I**) in *vastus lateralis* muscle obtained from human patients with HFpEF or PH-HFpEF. Data are mean ± SEM. Statistical comparisons were performed using Mann-Whitney *U*-test.

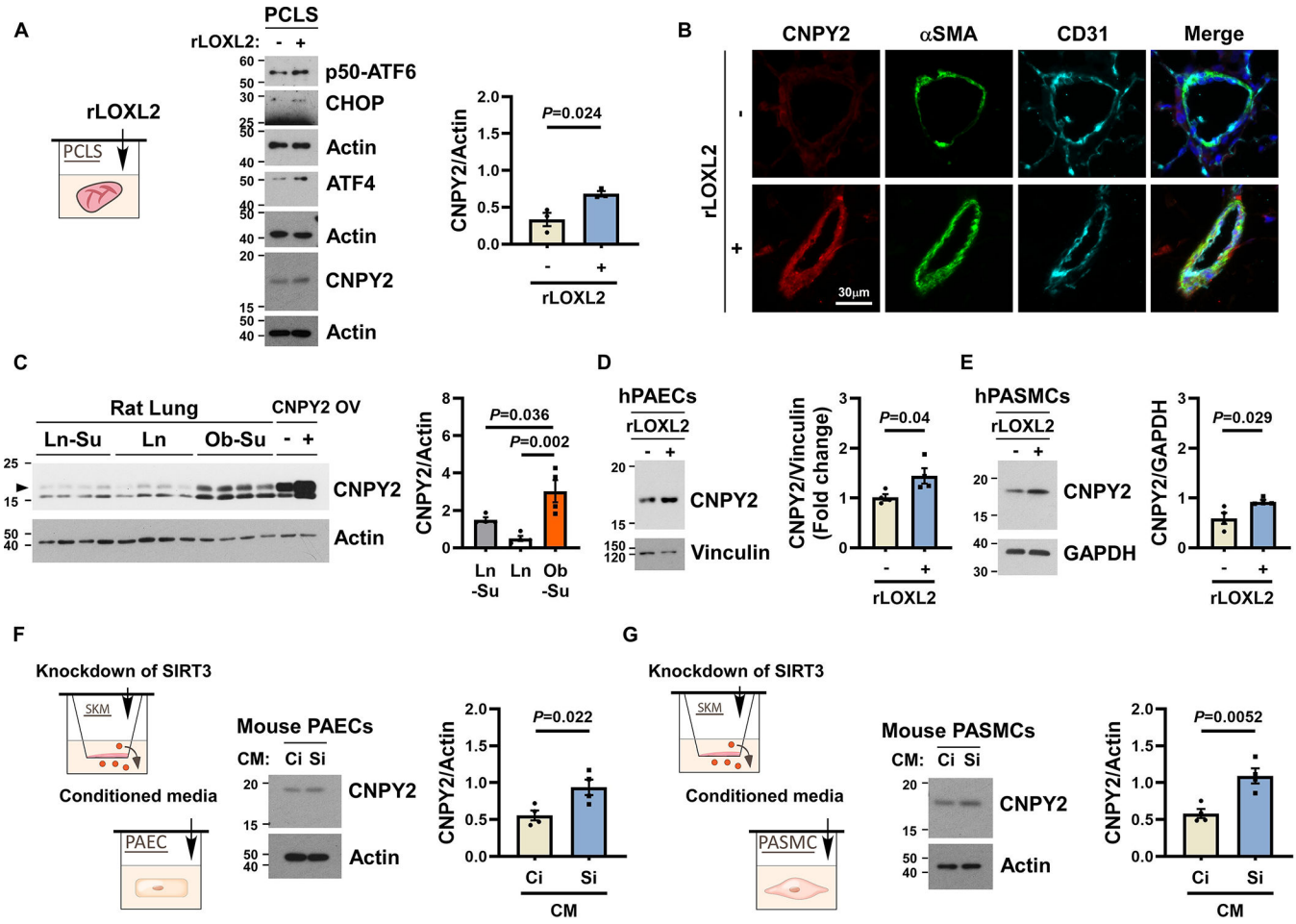

Figure 4.

Treatment with LOXL2 increases CNPY2 protein expression in PCLS, PAECs, and PASMCs. **A**, PCLS from C57B6 mice were treated with recombinant LOXL2 protein (500 ng/ml, labeled as "+") or vehicle control (labeled as "-") for 7 days. Representative images of Western blots for p50-ATF6, ATF4, CHOP, and CNPY2 protein expression levels in PCLS ($n = 3$). **B**, Representative images of PCLS stained with CNPY2 (red), α-smooth muscle actin (α-SMA, green), CD31 (light blue), and counterstained with DAPI (40X). **C**, Representative Western blots for CNPY2 protein expression levels in lungs of Ob-Su rats compared with lean rats ± SU5416 exposure (Ln and Ln-Su). **D** and **E**, Representative images of Western blots for CNPY2 protein expression levels in cultured human PAECs (**D**) and PASMCs (**E**) treated with recombinant LOXL2 protein (250 ng/ml, serum-free medium) for 2 days. **F** and **G**, C2C12 cells were differentiated to 70% confluence and transiently transfected with siRNA targeting SIRT3 or scrambled control for 72 hours. Conditioned media from scrambled control (labeled as "Ci") or SIRT3-deficient (labeled as "Si") C2C12 cells were treated to PAECs (**F**) or PASMCs (**G**) isolated from C57B6 mice for 2 days. CNPY2 protein levels were measured. Data are mean ± SEM. $n = 3$–4/group. Statistical comparisons were performed using unpaired Student's *t*-test after testing for normality with Shapiro-Wilk test. For Figure 4C, one-way ANOVA followed by Tukey's *post hoc* test was performed.

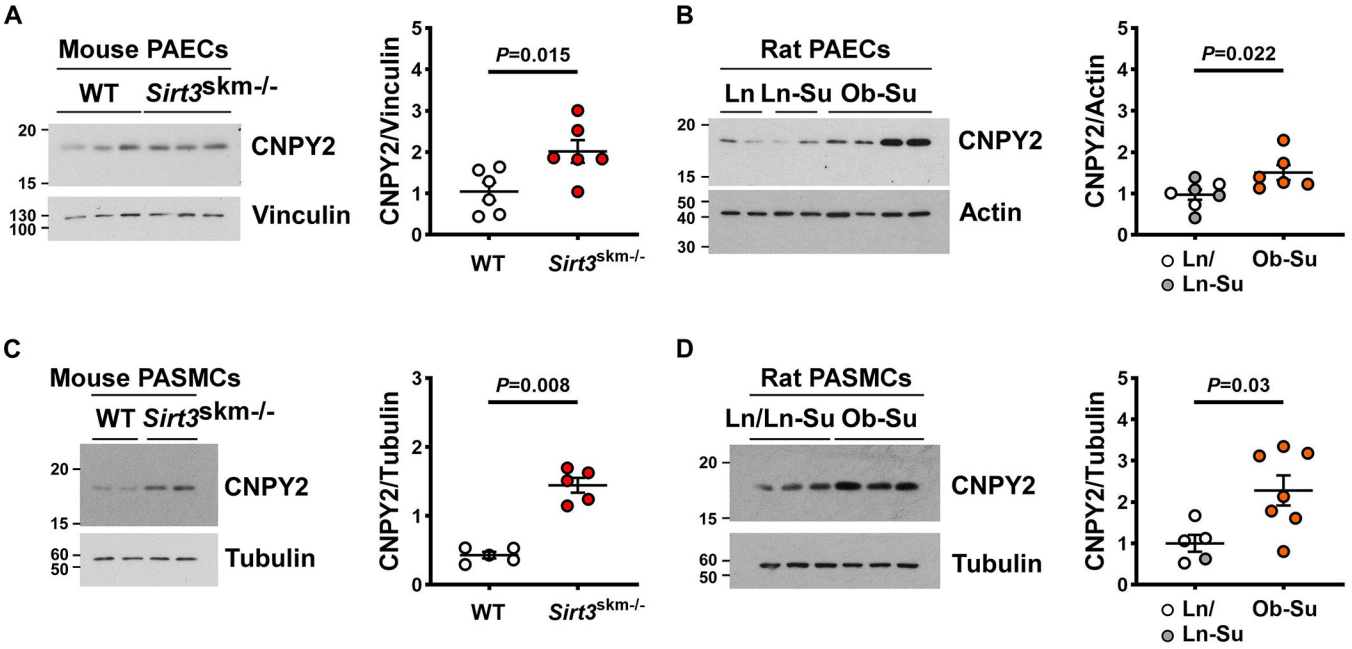

E

Sub	Age	Sex	BMI
1	35	M	29
2	58	M	20.8
3	38	M	25.6
4	38	M	26.5
5	70	M	22.9
6	53	M	20
7	61	M	38.3
8	43	M	39.5
9	53	M	39.5
10	40	M	31.1
11	34	M	46.2
12	47	M	32.5

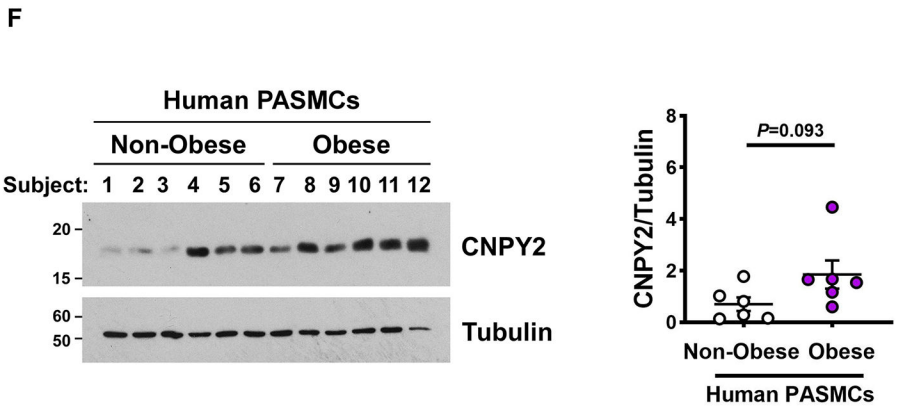

Figure 5.

Elevated CNPY2 expression in PAECs and PASMCs of *Sirt3*$^{skm-/-}$ mice and Ob-Su rats, and PASMCs of human subjects with obesity/diabetes. **A** and **B**, Representative Western blots for CNPY2 protein expression levels in PAECs of *Sirt3*$^{skm-/-}$ mice (**A**) and Ob-Su rats (**B**). **C** and **D**, Representative images of CNPY2 levels in PASMCs of *Sirt3*$^{skm-/-}$ mice (**C**) and Ob-Su rats (**D**). **E**, Clinical information for human PASMCs. **F**, Representative images of Western blots for CNPY2 protein expression levels in PASMCs obtained from humans with or without obesity (using BMI of 29 as a cut-off to define obesity). Data are mean ± SEM. Statistical comparisons were performed using Mann-Whitney *U*-test.

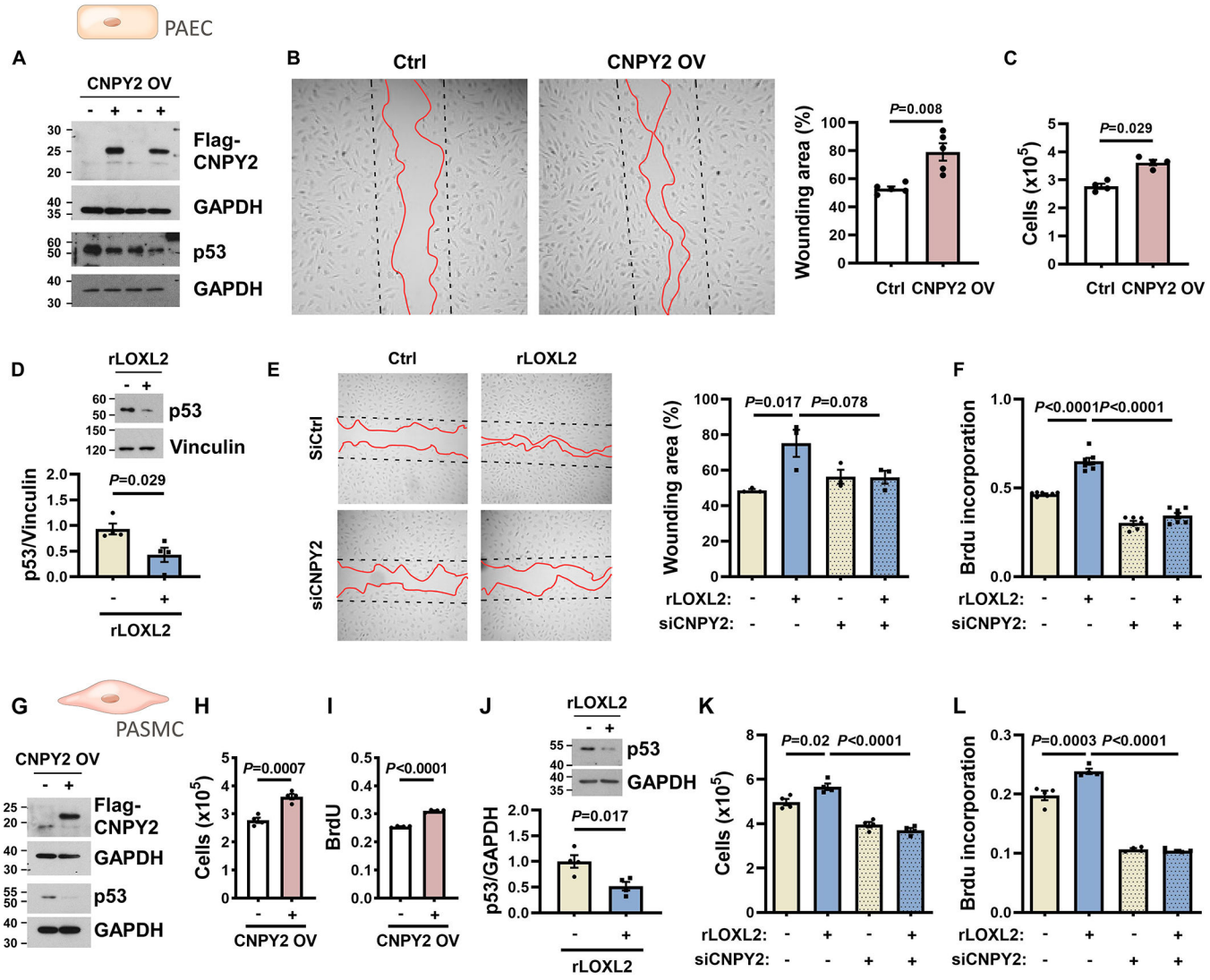

Figure 6.

Elevated CNPY2, either by overexpression or LOXL2 stimulation, promotes cell migration and proliferation. **A-C**, Cultured human PAECs were transfected with empty or CNPY2-expressing vector for 30 hours. Efficiency of CNPY2 overexpression and its effect on p53 were measured by Western blots (**A**). Representative images of wound closure and related quantitative data (**B**). Cell proliferation assessed by manual cell counts (**C**). **D**, Human PAECs treated with recombinant LOXL2 protein (250 ng/ml, serum-free medium) for 2 days. p53 expression levels were measured and quantified. **E** and **F**, Human PAECs were transiently transfected with siRNA targeting CNPY2 or scramble control before treatment with recombinant LOXL2 protein. Migration (**E**) and proliferation (**F**) of PAECs were measured. **G-I**, Human PASMCs were overexpressed with CNPY2 for 30 hours. Representative Western blots for CNPY2 and p53 protein levels (**G**). Cell proliferations measured by cell counts (**H**) and colorimetric BrdU incorporation (**I**). **J**, Human PASMCs treated with recombinant LOXL2 protein (250 ng/ml, serum-free medium) for 2 days. p53 expression levels were measured and quantified. **K** and **L**, Human PASMCs were

transiently transfected with siRNA targeting CNPY2 or scramble control for 24 hours before stimulation with recombinant LOXL2 protein (500 ng/ml, complete medium) for 5 days. Cell proliferation assessed by manual cell counts (**K**) and colorimetric BrdU incorporation (**L**). Data are mean ± SEM; n = 3–5/group. Statistical comparisons were performed using Mann-Whitney U-test, two-way ANOVA followed by Tukey's *post hoc* test, or unpaired Student's t-test after testing for normality with Shapiro-Wilk test.

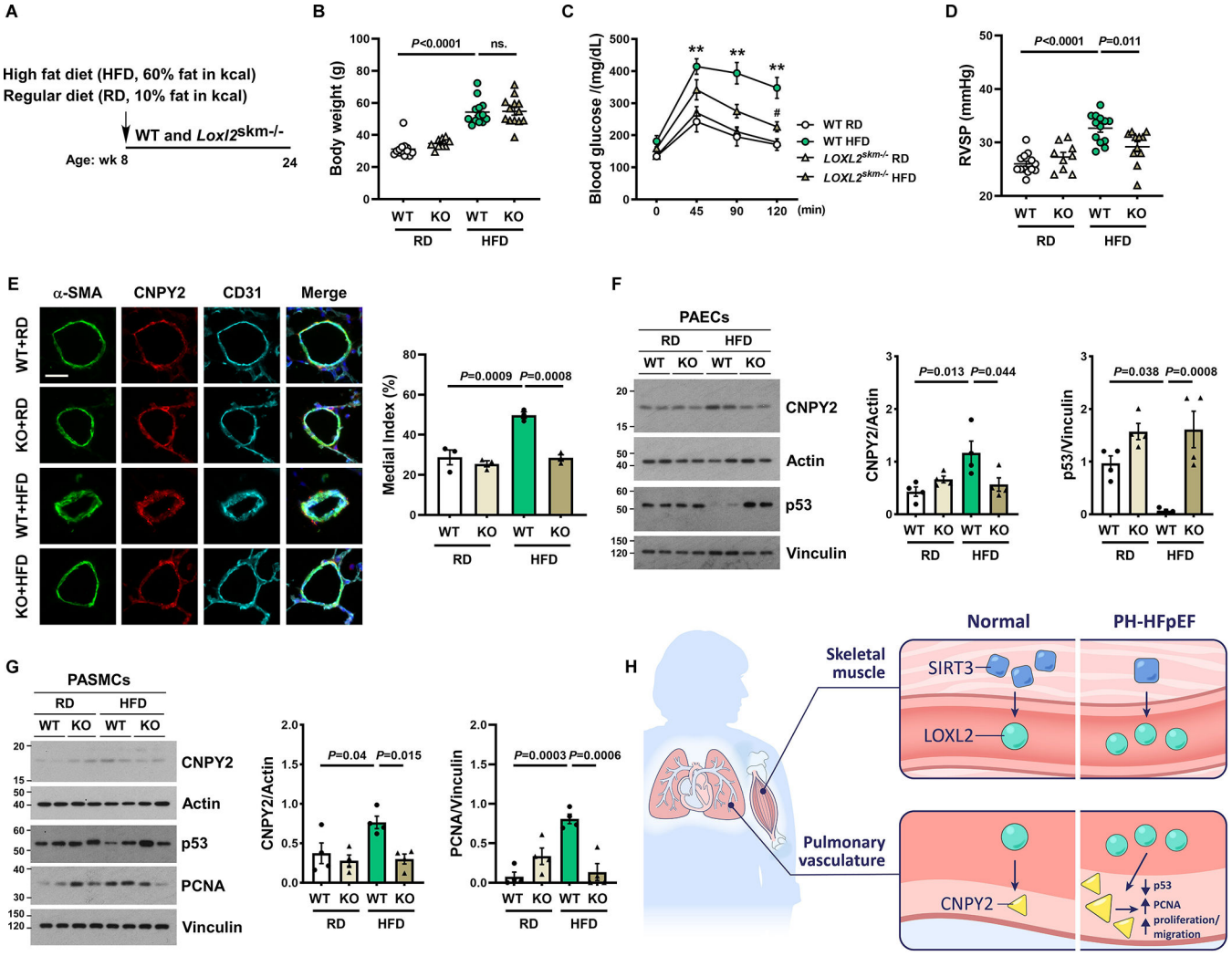

Figure 7.

Skeletal muscle-specific LOXL2 deletion reduces PAECs/PASMCs expression of CNPY2 and improves pulmonary pressures in mice with HFD-induced PH-HFpEF. **A**, Eight-week-old male *Loxl2*$^{\text{skm}-/-}$ and WT mice were fed with a HFD (60% lipids/kcal) or RD (10% lipids/kcal) for 16 weeks. **B**-**D**, Body weight (**B**), glucose tolerant abilities (**C**), and right ventricular systolic pressures (RVSP, **D**) were measured. **E**, Representative images of lungs stained with α-smooth muscle actin (α-SMA, green), CNPY2 (red), CD31 (light blue), and counterstained with DAPI (40X). *Scale bar*, 30 μm. Medial index was calculated. **F-G**, Representative Western blots and quantification of CNPY2, p53, or PCNA in PAECs (**F**) and PASMCs (**G**) isolated from WT and *Loxl2*$^{\text{skm}-/-}$ mice. **H**, Schema summarizing results relating skeletal muscle secretome to pulmonary vascular remodeling in PH-HFpEF. Statistical comparisons were performed using two-way ANOVA followed by Tukey's *post hoc* test. For Figure 7C, two-way ANOVA followed by Bonferroni's *post hoc* test was performed.